## Title

Secondary thalamic neuroinflammation after focal cortical stroke and traumatic injury mirrors corticothalamic functional connectivity



## Journal

The Journal of Comparative Neurology, 530(7)

## ISSN

1550-7149

## Authors

Necula, Deanna
Cho, Frances S
He, Andrea
et al.

## Publication Date

2022-05-01

## DOI

10.1002/cne.25259

Peer reviewed

HHS Public Access

Author manuscript

*J Comp Neurol*. Author manuscript; available in PMC 2023 May 01.

Published in final edited form as:

*J Comp Neurol*. 2022 May ; 530(7): 998–1019. doi:10.1002/cne.25259.

# Secondary thalamic neuroinflammation after focal cortical stroke and traumatic injury mirrors corticothalamic functional connectivity

**Deanna Necula**[1,2,3], **Frances S. Cho**[1,2,3], **Andrea He**[1], **Jeanne T. Paz**[1,2,3]

[1]Gladstone Institute of Neurological Disease, San Francisco, California, USA

[2]Neuroscience Graduate Program, University of California, San Francisco, California, USA

[3]Department of Neurology and the Kavli Institute for Fundamental Neuroscience, University of California San Francisco, San Francisco, California, USA

## Abstract

While cortical injuries, such as traumatic brain injury (TBI) and neocortical stroke, acutely disrupt the neocortex, most of their consequent disabilities reflect secondary injuries that develop over time. Thalamic neuroinflammation has been proposed to be a biomarker of cortical injury and of the long-term cognitive and neurological deficits that follow. However, the extent to which thalamic neuroinflammation depends on the type of cortical injury or its location remains unknown. Using two mouse models of focal neocortical injury that do not directly damage subcortical structures—controlled cortical impact and photothrombotic ischemic stroke—we found that chronic neuroinflammation in the thalamic region mirrors the functional connections with the injured cortex, and that sensory corticothalamic regions may be more likely to sustain long-term damage than nonsensory circuits. Currently, heterogeneous clinical outcomes complicate treatment. Understanding how thalamic inflammation depends on the injury site can aid in predicting features of subsequent deficits and lead to more effective, customized therapies.

### Keywords

astrocytes; microglia; neuroinflammation; *nucleus reticularis thalami* ; stroke; thalamus; traumatic brain injury

**Correspondence** Jeanne T. Paz, Gladstone Institute of Neurological Disease, San Francisco, CA 94158, USA. jeanne.paz@gladstone.ucsf.edu.

AUTHOR CONTRIBUTIONS

Conceptualization: D.N. and J.T.P.; Surgical procedures: D.N. and J.T.P.; Histology and imaging: D.N.; Data analysis: D.N., F.S.C., A.H., and J.T.P.: Writing—original draft: D.N and J.T.P.; Writing—review and editing: all authors; Funding acquisition: J.T.P.

COMPETING INTERESTS

The authors declare no competing interests.

DATA AVAILABILITY STATEMENT

The data that support the findings of this study are available from the corresponding author upon reasonable request.

PEER REVIEW

The peer review history for this article is available at https://publons.com/publon/10.1002/cne.25259.

## 1 | INTRODUCTION

Stroke and traumatic brain injury (TBI) are two of the leading causes of disability worldwide, with 13.7 million people experiencing a stroke and 69 million sustaining a TBI each year (Dewan et al., 2018; Lindsay et al., 2019). Fifty percent of patients hospitalized with TBI become permanently disabled, amounting to over 3 million individuals in the United States alone (Jourdan et al., 2018; Zaloshnja et al., 2008). Furthermore, while the majority of TBIs sustained in the United States are less severe concussive injuries, these milder events often lead to long-lasting functional impairments (Dean & Sterr, 2013). Likewise, 50–60% of patients experience lasting motor problems poststroke even with rehabilitation, and a comparable percentage require assistance with day-to-day tasks (Nascimento, 2021; Schaechter, 2004). In addition to stroke-related motor impairments, abnormal cognition, including attention and short-term memory deficits, often persists poststroke and can progress for years after the initial injury (Hochstenbach et al., 2003; Jourdan et al., 2018). Altogether, stroke and TBI are responsible for a host of neurological deficits with high burdens of disability, including cognitive impairments, motor abnormalities, psychiatric disorders, epilepsy, and sleep disruption (Centers for Disease Control & Prevention, 2015; Ferguson et al., 2010; Jourdan et al., 2018).

Despite the profound disease burden of both stroke and TBI, there is an acute shortage of available treatments. A major obstacle to effective therapeutic treatment is the heterogeneity of clinical outcomes; depending on various injury parameters, the nature and severity of clinical outcomes can vary widely. One source of variability is the site of injury. Studies have found that the nature of symptoms and the degree and longevity of disability both depend in part on where the injury was sustained (Gauthier et al., 2018; Kessner et al., 2019; Ohara et al., 2010; Sul et al., 2019). For cortical injuries, stroke or TBI centered in motor areas may selectively impair locomotion or dexterity, whereas injuries localized in the prefrontal cortex (PFC) may damage executive functioning but leave motor faculties largely intact (Liepert et al., 2005; Yuan & Raz, 2014). Therefore, a one-size-fits-all model of treatment may be ineffective for many patients. Furthermore, developing a better understanding of how lesion site dictates clinical outcomes could lead to targeted therapies designed to preempt anticipated long-term deficits.

There is mounting evidence that the thalamus, a remote subcortical region, may contribute to postinjury deficits (Cao et al., 2020; Dickerson et al., 2020; Grossman & Inglese, 2016; Grossman et al., 2012; Kuchcinski et al., 2017; Lutkenhoff et al., 2020; Sandsmark et al., 2017; Scott et al., 2015). Despite being insulated from the primary site of cortical injury, the ipsilateral thalamus exhibits intensifying secondary neuroinflammation even while the cortical inflammatory response associated with the primary injury abates. This phenomenon has been observed in both rodent models and human patients and has been associated with secondary thalamic neurodegeneration and neuroinflammation after TBI (Holden et al., 2021; Manninen et al., 2021; Ramlackhansingh et al., 2011; Scott et al., 2010), and after stroke (Cao et al., 2020; Kuchcinski et al., 2017; Langen et al., 2007; Pappata et al., 2000; Paz et al., 2010; Paz et al., 2013; Weishaupt et al., 2016).

Because the thalamus acts as a critical hub of neural activity, thalamic disruption is likely to have a wide-ranging impact on neurological function. Indeed, the thalamus has been implicated in a variety of secondary poststroke and TBI impairments in both rodent models and human patients, including cognitive dysfunction, sleep disruption, and sensory-perceptual errors (Cao et al., 2020; Grossman & Inglese, 2016; Grossman et al., 2012; Kuchcinski et al., 2017; Sandsmark et al., 2017). In particular, while moderate neuroinflammation may serve a neuroprotective function (Fraser et al., 2010), thalamic inflammation after TBI has been associated with sleep-wake disruptions (Hazra et al., 2014) as well as abnormal sleep spindles and epileptic activity (Manninen et al., 2021; Holden et al., 2021). Moreover, the degree of preservation of thalamic circuitry after cortical ischemia is a predictor of motor performance after TBI in humans (Binkofski et al., 1996). Similarly, secondary injury to the thalamus has been associated with sensory misperceptions and reduced verbal fluency in stroke patients (Cao et al., 2020). However, despite growing awareness of the role of thalamic inflammation in unfavorable clinical outcomes, no animal study has examined how the type and location of cortical injury influence the location of secondary thalamic inflammation.

Understanding how the site and type of cortical injury dictates thalamic inflammation may improve the predictive accuracy of clinical outcomes. Here, we investigated how the site and type of cortical injury modulates the location of inflammation in the thalamus. Specifically, we analyzed microglial and astrocytic activation as neuroinflammatory proxies in several thalamic subregions following cortical injury. Our results indicate that both cortical stroke and cortical TBI lead to the activation of microglia and astrocytes in the functionally connected regions of the relay thalamic nuclei and the *nucleus reticularis thalami* (nRT), and that sensory corticothalamic regions may be more likely to sustain secondary neuroinflammation than nonsensory circuits. Furthermore, first order thalamic nuclei were more likely to be inflamed than higher order thalamic nuclei. In sum, this work sets the stage for the design of therapies that can preempt or treat deficits influenced by region-specific thalamic neuroinflammation.

## 2 | MATERIALS AND METHODS

### 2.1 | Animals

All experiments were conducted per protocols approved by the Institutional Animal Care and Use Committee at the University of California, San Francisco and Gladstone Institutes. Precautions were taken to minimize stress and the number of animals used in each set of experiments. Adult (P40–P50) male C57BL/6 mice (ISMR_JAX: 000664) were used for the experiments. Five to eight mice were used per cortical site for each injury type. Altogether, 25 mice were subjected to TBI and 8 underwent the sham TBI surgery. Similarly, 25 mice were subjected to stroke and 8 underwent the sham stroke surgery. One V1 stroke mouse died postoperatively and was excluded from the study. One PFC TBI sham mouse was discovered to have hydrocephalus during brain sectioning and was excluded from the study.

### 2.2 | Controlled cortical impact (TBI)

Mice were weighed and anesthetized with 2–5% isoflurane, after which they were placed in a stereotaxic frame. TBI was performed after producing a 3 mm craniotomy centered over the following regions of the cerebral cortex: (1) primary visual cortex (V1) (centered at −2.9 mm posterior from bregma, +2.5 mm lateral from the midline, 10° angle); (2) primary somatosensory cortex (S1) (centered at −1 mm posterior from bregma, +3.5 mm lateral from the midline, 22° angle); (3) primary motor cortex (M1) (centered at +1.5 mm anterior from bregma, +1 mm lateral from the midline, 10° angle); and (4) anterior cingulate cortex region of the PFC (centered at +1 mm anterior from bregma, midline, 0° angle). With the exception of the injury to the PFC, which was bilateral over the midline, all impacts were delivered to the right hemisphere.

TBI was performed with a controlled cortical impact (CCI) device (Impact One Stereotaxic Impactor for CCI, Leica Microsystems) equipped with a metal piston using the following parameters: 3 mm tip diameter, depth 0.8 mm from the dura, velocity 3 m/s, and dwell time 100 ms. Sham animals received identical anesthesia and partial craniotomy (skull thinning) above the relevant cortical regions, but no injury.

### 2.3 | Photothrombotic cortical stroke

Mice were weighed and anesthetized with 2–5% isoflurane, after which they were placed in a stereotaxic frame. Photothrombosis was performed as described previously (Paz et al., 2010; Paz et al., 2013). After anesthesia, mice were injected with the light-sensitive Rose Bengal dye (40 mg/kg) (Sigma-Aldrich) intraperitoneally, and a 0.6 W light from a 3-mm-diameter Fiber-Lite MI-150 fiber optic cable was focused on the skull for 2 minutes. The optical system was designed to have an emission spectrum that encompassed the in vivo absorption range of Rose Bengal (maximum absorbance at 562 nm). To induce a focal photothrombotic lesion in the cortex, the light beam was centered using the same coordinates and angle as described above for the TBI induction, with the exception of the S1 injury, for which the mediolateral coordinate used for stroke induction was +4.5 mm. Control littermate mice received the same injection of Rose Bengal and identical anesthesia but were not photostimulated. With the exception of the injury to the PFC, which was bilateral over the midline, all strokes were induced in the right hemisphere.

### 2.4 | Immunostaining and microscopy

Mice were anesthetized with a lethal dose of Fatal-Plus and perfused with 4% paraformaldehyde in 1X PBS. Serial coronal sections (30 $\mu$m thick) were cut on a Leica SM2010R sliding microtome. Sections were incubated with antibodies directed against the glial fibrillary acidic protein (GFAP) (1:1000, chicken, Abcam, ab4674, AB_304558) and the ionized calcium binding adaptor molecule 1 (Iba1) (1:500, rabbit, Wako, 019–19741, AB_839504) overnight at 4°C. Blocking steps were performed in 10% normal goat serum (Jackson ImmunoResearch, 005–000-121). Primary antibodies were also diluted in 10% normal goat serum, while secondary antibodies were diluted in 3% normal goat serum. After wash, sections were incubated with Alexa Fluor conjugated secondary antibodies (1:1000 goat anti-chicken 488, ThermoFisher Scientific, A11039 (AB_142924), and 1:500 goat anti-rabbit 594, ThermoFisher Scientific, A11012 (AB_141359)) for 2 hours at room

temperature. Sections were mounted in an antifade medium containing DAPI (Vectashield) and imaged using a BZ-X710 Keyence microscope at 10×. Four to seven sections were stained per animal. High magnification images were obtained using a Zeiss LSM880 confocal microscope at 63× and represent maximum intensity projections of z-stacks.

### 2.5 | Antibody characterization

Antibodies were extensively characterized in previous studies in the Paz lab and elsewhere (see references below) using the appropriate controls (e.g., secondary antibody application without primary antibody). The antibodies were found to be robust and specific to their intended target(s).

The GFAP antibody was made against recombinant full-length human GFAP (1:1000, chicken, Abcam, ab4674, AB_304558) has been used extensively in previous reports (Ahn et al., 2021; Suarez-Mier & Buckwalter, 2015; Worker et al., 2020). Previous studies have validated its specificity by demonstrating that the antibody recognized cells with astrocyte morphology in controlled cocultures, and that antibody labeling of astrocytes coincided with genetic modes of astrocyte identification (Müller et al., 2015). Furthermore, our experiments demonstrated that the antibody-stained cells appeared consistent with typical astrocyte morphology.

The Iba1 antibody was purified in rabbit and made against the synthetic peptide C-terminal of Iba1 (1:500, rabbit, Wako, 019–19741, AB_839504). We found that at high magnification, Iba1 selectively stained cells with a typical microglial morphology. Prior RNA blot analyses have determined that Iba1 expression is highly restricted to microglia (Imai et al., 1996).

### 2.6 | Statistical analyses

All numerical values are given as means and error bars are standard error of the mean (SEM) with the exception of medians represented in the boxplots or unless stated otherwise. Extreme outliers beyond the outer fences of the boxes, defined as 3* interquartile range (IQR) below or above the first quartile or third quartile, respectively, were eliminated in an unbiased manner. Parametric and nonparametric tests were chosen as appropriate and are reported in figure legends. Trends were defined by $p$-values that became nonsignificant (>.05) only after correction for multiple comparisons. Data analysis was performed in the Python Integrated Development Environment Pycharm (SCR_018221), GraphPad Prism 9 (SCR_002798), and ImageJ (SCR_003070).

### 2.7 | Lesion severity quantification

Lesion severity was quantified by classifying the cortical injury on a 0–4 index scale (Figure 1a); 0: no cortical inflammation or cavity; 1: cortical inflammation (blue) but no cavity; 2: cortical inflammation and partial cavity; 3: cortical inflammation, loss of the entire cortical column at the lesion site, and near complete or complete cortical loss; and 4: damaged subcortical hippocampus in addition to the cortex (lesion severity of 0 is not pictured as the injury site appears identical to sham). For each section, cortical regions were identified using the Franklin and Paxinos mouse brain atlas (Paxinos & Franklin, 2007). To calculate

lesion severity, sections containing or near the maximum site of injury were selected along with impacted neighboring sections from each brain. We then averaged the maximum lesion severity of all mice in each given injury condition and injury type to obtain average maximum lesion severity. Presence or absence of cortical inflammation was determined both relative to cortical Iba1 and/or GFAP fluorescence seen in the contralateral hemisphere (where applicable), and relative to cortical Iba1 and/or GFAP fluorescence in sham mice.

### 2.8 | Image fluorescence analysis

Regions of interest (ROIs) were selected from 10× Keyence microscope images opened in ImageJ (SCR_003070) and manually identified using the Franklin and Paxinos mouse brain atlas. All analyzed brain sections were derived from coordinates −0.8 to −2.06 mm posterior from bregma. To ensure that each ROI covered the same area on the ipsilateral and contralateral sides of the injury site, the first ROIs were duplicated and repositioned over the opposite hemisphere wherever possible. To account for instances in which it was not possible to utilize the duplicated ROI on the contralateral hemisphere, all fluorescence results were normalized by the area of the ROI. To analyze fluorescence, the image was first converted to 8-bit. An integrated density ratio was calculated for each ROI by dividing the ipsilateral raw integrated pixel density by the contralateral raw integrated pixel density. For the PFC, because the injury was bilateral over the midline, the raw integrated pixel density of the ROIs in both hemispheres was averaged and divided by a “neutral” ROI elsewhere subcortically that did not show any inflammation in either sham or injured mice. For more anterior sections, this was approximately the nucleus reuniens of the thalamus, while for more posterior sections, this was approximately the periaqueductal gray (Figure 2). The integrated density ratios from 2 to 6 sections per animal were averaged to get a single average ratio per brain area for each animal.

## 3 | RESULTS

### 3.1 | The severity of the cortical injury depends on the site of impact

We first investigated the effect of stroke and TBI on injury severity in various cortical regions. Mice were subjected to either photothrombotic stroke (Paz et al., 2010, 2013), or the CCI model of TBI (Holden et al., 2021). Both injury models are considered to be focal and reproducible (Holden et al., 2021; Paz et al., 2013). The severity of cortical injury was assessed 1 week postinjury using a four-point index scale (Figure 1a). Stroke or TBI was centered at one of four cortical locations selected because of their dense reciprocal connections with distinct thalamic regions: the primary visual cortex (V1), the primary somatosensory cortex (S1), the primary motor cortex (M1), and the anterior cingulate region of the PFC (Figure 1b). All injuries were unilateral to the right hemisphere except for the PFC injury, which was applied to the midline and therefore bilateral.

Both stroke and TBI led to measurable cortical injury at each targeted site relative to sham controls (Figures 1b and 3). However, despite the use of identical injury parameters within each injury type, certain cortical injury sites led to more widespread damage. For example, V1 injury produced more total damage compared to M1 and PFC injury and appeared to more severely damage surrounding cortical areas (Figure 1c–e). Moreover, certain cortical

areas sustained more damage than others. Notably, both stroke and TBI administered to the V1 and S1 resulted in more severe cortical injury at the targeted site than injury aimed at the M1 and PFC. Indeed, on average, V1 and S1 cortices were more severely damaged than the M1 and PFC cortices 1 week after either photothrombotic stroke or TBI (Figure 1c). Together, these results suggest that some cortical areas are more susceptible to damage irrespective of whether the acute injury is a stroke or TBI. This variation in resilience to injury is presumably independent of anatomical variations in skull thickness, given that similar regional vulnerability to injury was observed in both craniotomized TBI mice and noncraniotomized stroke mice.

Although the injuries were largely focal, injury at one cortical site led to a gradient of damage in proximate regions that diminished in severity the more remote the region was from the site of injury. One exception was in the case of both PFC stroke and TBI, where the injury appeared more severe in the adjacent M1 cortex than in the PFC (Figure 1c,e), likely because of the close apposition of these two cortical regions.

### 3.2 | Secondary thalamic gliosis mirrors cortico-thalamic connectivity primarily in the visual and somatosensory circuits

To determine the extent to which the location of thalamic neuroinflammation depends on the site of cortical injury, we first assessed the presence of Iba1-positive reactive microglia in various thalamic regions 1 week after site-specific cortical injury (Figure 4) (Imai et al., 1996; Ito et al., 2001; Walker & Lue, 2015). We analyzed the raw integrated pixel density of Iba1 fluorescence as a proxy of microgliosis (Shapiro et al., 2009; Walker& Lue, 2015; Hopperton et al., 2018) in the thalamic regions most densely interconnected with the four injured cortical sites (see Methods). Each thalamic region was subdivided into constituent ROIs (Fama & Sullivan, 2015; Hwang et al., 2017; Nakajima & Halassa, 2017; Lindsay et al., 2019; Parnaudeau et al., 2018): (a) in the visual thalamus: the dorsal lateral geniculate nucleus (dLGN), lateral dorsal nucleus (LD), lateral posterior nucleus (LP), and nRT head; (b) in the somatosensory thalamus: the ventrobasal thalamic complex (VB), the posterior thalamic nucleus (Po), and the nRT body; (c) in the motor thalamus: the ventromedial nucleus (VM) and ventrolateral nucleus (VL); and (d) in the limbic thalamus: the mediodorsal nucleus (MD), central lateral thalamic nucleus (CL), and the nRT tail.

**3.2.1 | Injury centered on the V1—**Mice that had sustained a stroke in the V1 showed the strongest microgliosis in the visual thalamic nuclei 1 week poststroke relative to other thalamic nuclei (Figure 5a1). Microgliosis was observed in all excitatory thalamocortical nuclei (dLGN, LP, and LD) reciprocally connected with V1 and in the visual sector (head) of the GABAergic nRT (Figures 5a1 and 8a1). Notably, the microgliosis was specific to the visual sectors of the thalamus and not observed in somatosensory, motor, or limbic nuclei. Similarly, mice that had sustained TBI in the V1 had pronounced microgliosis in the same visual thalamocortical nuclei and the visual sector of the nRT 1 week postinjury. However, although V1 TBI resulted in the most robust microgliosis in the visual thalamic regions, it also produced mild microgliosis in somatosensory and motor thalami (Figure 5a2). This more diffuse thalamic microgliosis is unlikely to be a product of discrepancies in cortical

lesion severity between the two injury models, as both stroke and TBI led to a comparable degree of cortical damage (Figure 1d).

**3.2.2 | Injury centered on the S1—**Both stroke and TBI centered on the S1 led to microgliosis in the somatosensory excitatory first order and higher order thalamocortical relay nuclei (VB and Po, respectively), and the somatosensory sector of the GABAergic nRT (Figures 5b1, b2 and 7b1, b2). Although microgliosis was most robust in the somatosensory thalami, it was also observed to a lesser degree in the visual thalami in stroke but not TBI mice, in keeping with the greater damage to the V1 in stroke. Moreover, mice that had sustained S1 stroke had mild microgliosis in the motor thalamus (Figure 5b1).

**3.2.3 | Injury centered on motor and prefrontal cortices—**Mice with stroke or TBI centered on the M1 exhibited a trend toward selective microgliosis in the motor thalamus but not in visual, somatosensory, or limbic thalami. Of the motor thalamic nuclei, the VL appeared particularly inflamed, whereas the VM showed no signs of gliosis (Figure 5c1, c2). However, because the increased microgliosis in the broader motor thalamus in both stroke and TBI mice amounted only to a trend, it may suggest that the motor thalami may be more resistant to cortical injury-induced inflammation than the sensory visual and somatosensory thalami. No thalamic nucleus exhibited significant microgliosis after cortical injury centered on the PFC, though the motor thalamus showed signs of inflammation after both PFC stroke and TBI (Figure 5d1, d2). Across cortical injury sites, thalamic microgliosis in the visual and somatosensory thalami after V1 and S1 injury, respectively, appeared to scale more closely with lesion severity compared to motor and limbic thalamus inflammation after M1 and PFC injury (Figure 5e1–e4). The microgliosis data per injury site for stroke and TBI are summarized in Figure 5f and 5g, respectively.

Next, we assessed the presence of reactive astrocytes, or astrogliosis, with the reactive astrocyte marker GFAP (Hol & Pekny, 2015). As with Iba1, GFAP fluorescence was selectively increased in the visual thalamus following V1 TBI and trended toward specificity to the visual thalamus after V1 stroke (Figure 6a1, a2). While the overall effect was of selective visual thalamus astrogliosis, no one thalamic nucleus had significant astrogliosis relative to sham for either injury type, though the LD, dLGN, and nRT head trended toward astrogliosis in stroke and TBI mice (Figure 6a1, a2).

Following S1 stroke, astrogliosis appeared in the somatosensory thalamus but only trended toward somatosensory selectivity after TBI (Figure 6b1, b2). The limbic thalamus exhibited increased astrogliosis after M1 TBI (Figure 6c2), but no thalamic nucleus was selectively inflamed after either stroke or TBI to the PFC (Figure 6d1, d2).

Altogether, these results suggest that astrogliosis may serve as a marker of cortical injury-induced inflammation 1 week postinjury, though it appears to be a less reliable inflammatory marker than microgliosis, at least at that timepoint. Across cortical injury sites, thalamic astrogliosis in the visual and somatosensory thalami after V1 and S1 injury, respectively, appeared to scale more closely with lesion severity compared to motor and limbic thalamus astrogliosis after M1 and PFC injury (Figure 6e1–e4). The microgliosis data per injury site for stroke and TBI are summarized in Figure 6f and 6g, respectively.

### 3.3 | The effect of cortical injuries on activation of microglia and astrocytes in the nRT

The nRT provides the main GABAergic input to all thalamocortical nuclei and regulates cortico-thalamo-cortical interactions involved in perception, sensation, sleep, consciousness, and attention (Campbell et al., 2020; Crabtree, 2018; Gentet & Ulrich, 2003; Halassa & Acsády, 2016; Houser et al., 1980; Lam & Sherman, 2011; McCormick & Bal, 1997; Reinhold et al., 2015; Sherman & Koch, 1986; Vantomme et al., 2019). Because of the critical role of the nRT in orchestrating electrical activity in the brain, disruptions in the nRT are associated with various neurological and psychiatric disorders (Paz et al., 2010; Paz et al., 2011; Ahrens et al., 2015; Hazra et al., 2016; Holden et al., 2021; Ritter-Makinson et al., 2019; Wells et al., 2016; Makinson et al., 2017). To determine more precisely how this key structure affects the site of thalamic inflammation secondary to cortical injury, we examined the effects of stroke and TBI on the location of neuroinflammation in various sectors of the nRT. The nRT can be roughly subdivided into three components with distinct functional specializations: the head, which connects to the visual thalamocortical nuclei (Campbell et al., 2020; Hoseini et al., 2021), the body, which connects to the somatosensory thalamocortical nuclei (Clemente-Perez et al., 2017; Lam & Sherman, 2011), and the tail, which connects to the limbic thalamocortical nuclei and to a lesser extent the motor thalamus (Crabtree, 2018; Lozsadi, 1994; Zikopoulos & Barbas, 2006; Cornwall et al., 1990; Lee et al., 2019; Zikopoulos & Barbas, 2012). The nRT also receives cortical projections that are topographically segregated according to the function of their cortical origin (Crabtree, 1992; Lam & Sherman, 2011).

We first analyzed microgliosis in the nRT 1 week after stroke or TBI. As in the relay thalamocortical nuclei, V1 stroke or TBI led to selective microgliosis in the head of the nRT (Figure 7a1, a2) (Campbell et al., 2020; Holden et al., 2021). Mirroring the more widespread microgliosis seen in the relay thalamocortical nuclei after V1 TBI relative to V1 stroke (Figure 5a1, a2), the body and tail of the nRT also showed signs of microgliosis, though Iba1 fluorescence quantification failed to reach statistical significance (Figure 7a1, a2). The widespread microgliosis seen in thalamocortical nuclei after S1 stroke and S1 TBI was also recapitulated in the nRT, with marked microgliosis seen across the head, body, and tail (Figure 7b1, b2).

Lastly, M1 TBI tended to cause increased microgliosis in the nRT body and tail (Figure 7c2), while we observed no signs of microgliosis in the nRT after PFC injury (Figure 7d1, d2). As in the thalamocortical nuclei, microgliosis in the head and body of the nRT after V1 and S1 injury, respectively, appeared to scale more closely with lesion severity compared to microgliosis in the nRT tail after M1 and PFC injury (Figure 7e1–e4). The microgliosis data per injury site for stroke and TBI are summarized in Figure 7f and 7g, respectively. In each injury setting, astrogliosis appeared in the same nRT sectors as did microgliosis (with some exceptions) (Figure 8), suggesting that cortical injuries lead to secondary activation of both microglia and astrocytes in the areas of the nRT that receive input from the damaged cortical and secondarily damaged thalamocortical regions. Astrogliosis, while still roughly adhering to patterns of functional connectivity, appeared less robust than microgliosis. The mild astrogliosis in the nRT following cortical injury was comparable to results in the relay thalamocortical nuclei, where postinjury astrogliosis was present but weak. As with

microgliosis, injury to the PFC did not result in astrogliosis in the nRT (Figure 8d1, d2). In contrast to microgliosis in the nRT, astrogliosis in the head and body of the nRT after V1 and S1 injury, respectively, did not appear to scale as closely with lesion severity (Figure 8e1–e4), suggesting again that astrogliosis may be a weaker marker of thalamic secondary injury at the 1 week timepoint. The astrogliosis data per injury site for stroke and TBI are summarized in Figure 8f and 8g, respectively.

These results indicate that the nRT, like the relay thalamocortical nuclei, is vulnerable to cortical injury-induced inflammation. Furthermore, regional inflammation in the nRT tends to follow the functional connectivity between the nRT, the relay thalamocortical nuclei, and the cerebral cortex.

### 3.4 | Secondary thalamic inflammation in first and higher order thalamic nuclei

Analysis of both higher order and lower order thalamic nuclei revealed that higher order thalamic nuclei tended to be less gliotic than first order thalamic nuclei (motor thalamus: first order, VL, higher order, VM; limbic thalamus: higher order, MD and CL) (Bennett et al., 2019; Gulcebi et al., 2012; Mitchell, 2015; Hoerder-Suabedissen et al., 2018; Perry & Mitchell, 2019; Ramcharan et al., 2005a) (Figure 9). This relationship appeared to be preserved particularly in mice subjected to V1 and S1 stroke (comparing dLGN vs. LD/LP, VB vs. Po, respectively) and examined for Iba1 fluorescence (Figure 9b). Moreover, microgliosis of the higher order regions of the visual and somatosensory thalami appeared to depend on lesion severity (Figure 9b). In contrast, the higher order regions in the motor and limbic thalami unilaterally showed mild or absent microglial activation, even when the injury was severe, though low sample size nullified statistical comparisons (Figure 9b,c). Similar findings were observed in the case of astrogliosis in the nRT; in both stroke and TBI mice, the gliosis appeared to scale with lesion severity for V1 and S1 injuries but remained mild for more severe M1 and PFC injuries (data not shown). Note that when the higher order/first order comparison was performed for each cortical injury site independently, all comparisons were insignificant (data not shown).

No matter the injury severity, there was no detectable V1 injury-associated micro- or astrogliosis in the ventral lateral geniculate nucleus (vLGN), a thalamic nucleus that has highly distributed connectivity similar to that of a higher order nucleus, though unlike a higher order nucleus, it does not project to the cortex (Figure 9d).

Altogether, the ratio of microgliosis was greater in first order nuclei than in higher order nuclei (Figure 9a). The apparent neuroprotective influence in higher order thalamic nuclei was not as conspicuous with astrogliosis (Figure 9a), consistent with astrogliosis being a less robust marker of secondary thalamic inflammation 1 week after injury.

## 4 | DISCUSSION

In this study, we sought to determine how the site and type of cortical injury influences the location of secondary thalamic micro- and astrogliosis, considered proxies for neuroinflammation. We show that cortical stroke and TBI both lead to secondary activation of microglia and astrocytes in regions of the thalamus known to be topographically

connected to the injured cortical site. This was particularly true for visual and somatosensory circuits, where injury to the V1 and S1 cortices led to selective activation of microglia and astrocytes in the visual and somatosensory relay thalamocortical nuclei, respectively, as well as in corresponding functional sectors of the GABAergic nRT.

Our findings in the photothrombotic stroke model mirror those from prior studies in rats and human patients with cortical stroke. Previously, two groups independently found that cortical ischemia led to regionally-selective inflammation and neurodegeneration in the relay thalamus (Kuchcinski et al., 2017; Langen et al., 2007). However, these studies made no comparison between injury types. Furthermore, their assessment of thalamic inflammation and neurodegeneration relied predominantly on indirect measures like iron accumulation and positron emission tomography tracer uptake, and they focused on characterizing thalamic retrograde neurodegeneration more than on quantifying thalamic inflammation (Kuchcinski et al., 2017; Langen et al., 2007). Our study built on this foundation to demonstrate a reproducible effect apparent by analysis of multiple neuroinflammatory markers across multiple injury types.

### 4.1 | Secondary thalamic inflammation is determined by cortical connections to first or higher order nuclei

The finding that injuries in the primary sensory cortical regions (V1 and S1) led to stronger glial activation in the thalamus than injuries in the nonsensory cortical areas (M1 and PFC) suggests that thalamic neuroinflammation follows certain rules of cortico-thalamo-cortical connectivity (Figures 5 and 6). One such “rule” may rely on the anatomical distinctions between first and higher order thalamic nuclei.

First order and higher order thalamic nuclei differ along a variety of functional and electrophysiological readouts, including firing patterns, source of driving input, and synapse number (Ramcharan et al., 2005; Bickford et al., 2015; Guillery, 1995; Sherman & Guillery, 1996; Sherman & Guillery, 2006; Van Horn & Sherman, 2007; Sherman & Guillery, 2013). First order thalamic nuclei receive sensory input from peripheral sensory receptors to relay to the cortex, receive inputs from a select few drivers, and have narrower outputs to the cortex (Sherman, 2007; Bickford et al., 2015; Sherman, 2016). In contrast, higher order nuclei are more widely connected across the cortex and are thought to act as conduits between different cortical areas (Sherman, 2007; Sherman & Guillery, 2002; Lee, 2013, Zimmerman & Grace, 2018).

Notably, comparison of inflammation at first and higher order nuclei suggested that higher order nuclei tend to show less inflammation than the first order nuclei (Figure 9a). We propose that the broader connectivity between higher order thalamic nuclei and the cortex relative to first order thalamic nuclei may explain why higher order nuclei appear more robust to injury; injury to an isolated cortical region would spare more of the connections to higher order nuclei.

It is worth noting that the higher order nuclei of the visual thalamus (LP and LD) and somatosensory thalamus (Po) were inflamed after V1 and S1 injuries respectively, in contrast to nonsensory nuclei like the MD. This may be because the V1 and S1 injuries

were on average more severe than the M1 and PFC injuries (Figure 1c,d), and so overcame the neuroprotective mechanisms that would have spared the higher order nuclei under milder injury conditions.

Some first order nuclei also share connectivity patterns with higher order nuclei, possibly protecting them from more severe secondary damage. For example, the VL, which is part of the motor thalamus, is alternately considered a first order nucleus because of its widespread subcortical/cerebellar/tectal inputs, or a higher order nucleus because of its diffuse cortical connectivity (Bosch-Bouju et al., 2013; Hwang et al., 2017; Sherman, 2016). However, while the VL does appear to exhibit some characteristics typical of higher order thalamic nuclei, namely, the relay of intercortical information, it is more often considered a first order nucleus given the predominance of subcortical inputs (Hwang et al., 2017; Power & Looi, 2015; Puelles et al., 2012). Because of the dense connectivity of VL with the cortex, it is not surprising that the VL exhibited mild but consistent microgliosis following injury to the M1. That the VL did not have any measurable astrogliosis postinjury may be due to astrogliosis being a weaker marker of thalamic inflammation, at least at the 1 week postinsult timepoint of our study. Indeed, prior studies have reported that astrocytes adopt a reactive state and are recruited to inflammatory sites largely in response to microglial signaling, implying that microgliosis precedes astrogliosis and thus may upstage astrogliosis at early timepoints. However, the weaker astrogliosis could also be explained by the VL's relative resilience as a putative first order nucleus, or by technical idiosyncrasies (e.g., differences in antibody efficacy) (Rosa et al., 2021; Zhang et al., 2010).

We speculate that first order thalamic nuclei are more vulnerable to focal cortical injury, perhaps because they adhere to the adage of "having all their eggs in one basket." In other words, the more widespread connections of higher order nuclei render them more resilient to cortical injury, be it stroke or TBI, while the more narrowly connected first order nuclei remain highly susceptible. That said, we cannot exclude the possibility that the differential vulnerability of sensory and non-sensory circuits may be a stronger determinant for secondary thalamic inflammation given that the nonsensory motor and limbic regions appeared overall more resilient to gliosis than the sensory visual and somatosensory regions.

### 4.2 | Potential role of retrograde versus anterograde degeneration in the development of secondary inflammation in the thalamus

First order and higher order thalamic nuclei also differ in the directionality of their inputs. Therefore, differences in the likelihood of injury-induced anterograde or retrograde degeneration may contribute to the unique vulnerability of first order nuclei to postinjury gliosis. While the field has acknowledged the role of anterograde degeneration in injury-induced thalamic astro- and microgliosis, most studies tend to implicate retrograde degeneration of thalamocortical connections as the primary source of thalamic inflammation after cortical injury (Langen et al., 2007; Lifshitz et al., 2007; Ross & Ebner, 1990; Sorensen et al., 1996). We found that thalamic regions for which the first order nuclei were analyzed, meaning those with a higher proportion of thalamocortical projections than corticothalamic projections, showed more inflammation post injury than thalamic regions for which higher order or semi-higher order nuclei like the VL (those with a higher proportion

of corticothalamic projections) were analyzed. This indicates that retrograde degeneration may indeed contribute more to thalamic inflammation after cortical injury compared to anterograde degeneration. However, it does not preclude the possibility that anterograde degeneration also plays a role in this inflammatory process, particularly since higher order nuclei have broader cortical connectivity in addition to more abundant thalamocortical projections, and so are expected to be more resilient to inflammation independent of the direction selectivity of degeneration.

Notably, in mice with V1 stroke or TBI, there was no detectable inflammation in the vLGN (Figure 9d), a thalamic nucleus that only receives cortical input and does not project to the cortex (Monavar-feshani et al., 2017). This suggests that anterograde degeneration is a weaker contributor to postcortical injury-induced thalamic inflammation than retrograde degeneration. However, the vLGN also receives input from a wider variety of brain regions and proportionally less cortical input relative to the dLGN, raising the possibility that the lack of gliosis in the vLGN reflects protection mediated by distributed connectivity, as observed in higher order thalamic nuclei.

Postinjury inflammation in the nRT may be due in part to anterograde degeneration (i.e., loss of cortical and thalamic inputs) given that the nRT does not project directly to the cortex (Crabtree, 1992; Lam & Sherman, 2011). However, postinjury gliosis in the nRT may also be a product of retrograde injury in the gliotic target relay thalamocortical nuclei to which nRT is intimately connected (Paz et al., 2010).

The nRT sends GABAergic inputs to the thalamocortical nuclei in a manner that mirrors the topographical organization of thalamocortical circuits. For example, the head of the nRT is thought to modulate visual information because it projects to the dLGN (Campbell et al., 2020; Hoseini et al., 2021). Similarly, the body of the nRT is primarily devoted to somatosensory processing and projects to first and higher order somatosensory thalamic nuclei, while the tail is considered a prefrontal or limbic center and contains neurons that project to higher order limbic thalamic nuclei, with some role in motor processing (Crabtree, 2018; Zikopoulos & Barbas, 2006; Collins et al., 2018). Our results indicate that nRT inflammation follows the topographical and functional organization that exists between the cortex, nRT, and the relay thalamus. Most telling is the selective micro- and astrogliosis of the head of the nRT in V1-injured mice. The nRT body, while exhibiting more widespread inflammation due to cortical injury overlap with adjacent regions, also tended to show enhanced micro- and astrogliosis following damage to S1 (Figures 7 and 8).

As with the thalamocortical nuclei, patterns of inflammation in the nRT following M1 and PFC injury remain inconclusive, although we found that the tail of the nRT does tend to become inflamed after M1 TBI, consistent with its role in motor processing (Crabtree, 2018). However, this result was not seen following M1 stroke, suggesting that the two injury types, although parallel in many respects, differ in their downstream cellular effects. The lack of robust gliosis in nRT after both M1 and PFC injuries may be a result of weak inflammation in connected areas of the thalamocortical nuclei. For example, injury to the V1 cortex that leads to severe gliosis in the dLGN may lead to selective gliosis in the head of the nRT, as the projections linking the nRT head and dLGN are adversely affected by dLGN

inflammation. It is therefore plausible that the absence of gliosis in the nRT tail following PFC injury is a product of the lack of robust inflammation in the associated limbic thalamus.

In sum, postcortical injury inflammation seen in the relay thalamus appears to depend more on retrograde degeneration than anterograde degeneration. However, future studies quantifying neuronal loss are required to determine the role of anterograde and retrograde degeneration in secondary thalamic inflammation.

### 4.3 | Certain cortical regions show enhanced susceptibility to long-term damage

Interestingly, while focal TBI and stroke led to cortical damage in all impacted areas, the severity of the damage in M1 and PFC was milder on average than the severity of lesions to the S1 and V1 cortices. This protective effect was particularly pronounced for the PFC, for which the average maximum lesion severity was especially mild. However, as mentioned earlier, it is unlikely that patterns of inflammation seen in the motor and limbic thalami are merely products of smaller lesions in their respective cortical connective partners, given that even severe injury to M1 and PFC cortices produced little to no thalamic inflammation, particularly in higher order thalami (Figure 9b,c).

Because the injury models were highly controlled, variability in lesion severity within each cortical injury site and injury type was low. As a result, we were unable to comprehensively assess the relationship between lesion severity and thalamic inflammation for injury of each type and at each site. However, as mentioned, our data suggest that even relatively severe lesions in the M1 and PFC do not produce notable differences in microgliosis in thalamocortical nuclei, in contrast to V1 and S1 injuries (Figure 9b,c). Therefore, it appears that the differences in resilience seen between cortical injury sites hold independent of lesion severity, though our experimental numbers were low. Ideally, future studies more directly investigating the spatial dependencies of cortical lesion severity should test lesion severity as an independent variable.

Though we do not suspect that the difference in lesion severity at various cortical lesion sites greatly impacted the degree of thalamic inflammation observed, the finding that the M1 and PFC injuries tended to produce milder cortical lesions despite the use of identical injury parameters as the V1 and S1 injuries is intriguing. One potential explanation is that these cortical regions are more resilient to acute injury or long-term damage. Alternatively, technical differences in the disease models may result in milder lesions in these areas than in the sensory cortices. Both possibilities are discussed below.

**4.3.1 | Resilience—**There is little precedent to suggest that the M1 and PFC are more resistant to injury than sensory cortices, but most previous studies have not systematically compared the effect of TBI or stroke on lesion severity across different cortical regions. However, one study found that small variations in the site of fluid percussion injury (FPI), another common form of experimental TBI, can lead to profound differences in both anatomical destruction and behavioral readouts (Floyd et al., 2002). This study induced FPIs in rats at rostral, caudal, medial, and lateral cortical coordinates using identical injury parameters, and showed that mortality was particularly high for animals that had received a caudal FPI and low for animals that had received a rostral FPI, suggestive of a potential

neuroprotective effect limited to the rostral brain. At the cellular level, hippocampal neuronal loss was far less pronounced in the rostral group relative to all other groups, and did not differ from that in the sham group. Moreover, the hippocampus of the caudal, medial, and lateral groups had significantly more reactive astrocytes than that of the rostral group. These cellular effects appeared to translate to behavior; mice subjected to rostral injury performed better on the hippocampus-dependent Morris water maze task than their caudally, medially, and laterally injured counterparts (Floyd et al., 2002). This study lends support to our findings that the rostral regions of the cortex (in our study, the M1 and more so the PFC) appear to benefit from some kind of neuroprotective influence.

Because of the short timescale of these experiments (tissue was collected a week after injury), it is unlikely that injuries in the PFC and M1 recovered so rapidly that the cavities disappeared or dramatically diminished in size before analysis. We can also discount this particular explanation because lesion size has been shown to increase over short timescales as cell loss intensifies (Loane et al., 2014). Rather, it is more likely that these regions were protected at the time of injury, or, more plausibly, that they were protected from the postinjury progressive increase in lesion size seen in other cortical regions (Loane et al., 2014).

Because few studies directly compare lesion severity and neuroinflammation at different injury sites, it is completely unknown what molecular/cellular events may underlie this neuroprotective effect. However, multiple factors could be at play. For example, previous studies have highlighted the vast transcriptional, morphological, and functional heterogeneity within glial cell types, and in particular within astrocyte and microglia populations in both rodents and humans (Masuda et al., 2020; Matias et al., 2019; Xin & Bonci, 2018; Liddelow et al., 2017; Escartin et al., 2021; Khakh & Sofroniew, 2015; Rose & Kirchhoff, 2015; Rosenberg & Molofsky, 2020). This remarkable diversity is highly brain region-specific (Matias et al., 2019; Masuda et al., 2020), making it not only possible but very likely that certain regions are rendered more or less vulnerable as a result of site-specific functional differences in glial behavior. These differences include but are not limited to variations in metabolic support, maintenance of blood–brain barrier integrity, and phagocytic activity. For example, astrocytes in various hippocampal regions have to be shown to differentially modulate neuronal activity (Khakh & Sofroniew, 2015), while thalamic microglia appear to have higher surface expression of immune markers compared to microglia residing in the temporal and frontal lobes (Böttcher et al., 2019). Moreover, it is well known that regional neuronal populations can be uniquely susceptible to injury and disease. For example, neurons in the hippocampus and subiculum are particularly prone to damage in Alzheimer’s disease (Matias et al., 2019). Differences in the orientation and distribution of vasculature have been also found in motor and integrative regions relative to sensory regions, which are properties known to influence recovery after ischemia and TBI (Kirst et al., 2020). However, it is unclear how this neuroprotective influence might depend on injury type.

### 4.4 | Technical considerations

We cannot exclude the possibility that the milder injury in the M1 and in particular the PFC cortices was due to technical aspects. In a previous study, induction of a cavitated and highly localized infarct in the PFC resulted in substantial microgliosis in the MD, suggesting that PFC injuries can lead to activation of microglia in the functionally connected limbic thalamus, and that inflammatory outcomes may be a product of the specificity, severity, and nature of the injury rather than the position (Weishaupt et al., 2016).

Our results cannot be explained by differences in skull thickness over the M1/PFC relative to more caudal regions of the brain, because we observed similar patterns following TBI and stroke, yet TBI mice were craniotomized such that the impact could be delivered directly to the cortex. Identical injury parameters were also used between cortical injury sites, making other technical discrepancies unlikely.

## 5 | CONCLUDING REMARKS AND FUTURE DIRECTIONS

Our study systematically compared the activation of thalamic microglia and astrocytes in two very different models of cortical injury: stroke and TBI. Both injury types led to similar patterns of thalamic inflammation, with thalamic micro- and astrogliosis mirroring the functional connectivity of cortico-thalamo-cortical circuits independent of injury type. This study provides evidence that the thalamus responds similarly to cortical TBI as it does to cortical stroke. These results suggest that treatments that target thalamic inflammation for stroke-related deficits may also be effective for TBI-related deficits, vastly expanding the therapies available for two of the leading causes of disability worldwide (Lindsay et al., 2019; Dewan et al., 2018).

While these results advance our understanding of the cellular events that occur in the thalamus after stroke and TBI, they do not address how these inflammatory processes might underlie behavior and injury-related impairments. Nevertheless, as we develop an increasing awareness of how thalamic inflammation might give rise to or modulate injury-induced deficits, it is imperative that we dedicate future studies to examining the implications of site-specific thalamic gliosis. The site of cortical injury affects a patient's outcome and the choice of therapeutic intervention (Kinnunen et al., 2011; Stocchetti & Zanier, 2016). However, the relative contribution of selective thalamic inflammation to clinical outcome versus that of the direct cortical injury is unknown. Rigorously examining the role of thalamic inflammation in behavioral deficits, cognitive impairments, and other injury-associated phenotypes would enable us to design effective and customized therapies that address a critical treatment gap.

## ACKNOWLEDGMENTS

We thank Irene Lew for assistance with animal husbandry, surgeries, and perfusions. We also thank Kathryn Claiborn for critical feedback on our manuscript, Jeremy Ford for helpful discussions, Sarah Gardner for graphic design contributions, and Gabe Jackman from the Keyence Corporation for invaluable microscopy assistance.

FUNDING

J.T.P. is supported by Gladstone Institutes. NIH/NINDS grants R01 NS096369, R21 NS118379. U.S. Department of Defense grants W81XWH1610576 and W81XWH2010160. D.N. is supported by the Hillblom/BariARI graduate fellowship. F.S.C. is supported by NINDS F31 NS111819–01A1.

Funding information

Gladstone Institutes; U.S. Department of Defense, Grant/Award Numbers: W81XWH1610576, W81XWH2010160; National Institute of Neurological Disorders and Stroke, Grant/Award Numbers: R01 NS096369, R21 NS118379, F31 NS111819–01A1; Hillblom/BARI graduate fellowship

## REFERENCES

Ahn LY, Coatti GC, Liu J, Gumus E, Schaffer AE, & Miranda HC (2021). An epilepsy-associated ACTL6B variant captures neuronal hyperexcitability in a human induced pluripotent stem cell model. Journal of Neuroscience Research, 99(1), 110–123. 10.1002/jnr.24747 [PubMed: 33141462]

Ahrens S, Jaramillo S, Yu K, Ghosh S, Hwang G-R, Paik R, Lai C, He M, Huang ZJ, & Li B (2015). ErbB4 regulation of a thalamic reticular nucleus circuit for sensory selection. Nature Neuroscience, 18(1), 104–111. 10.1038/nn.3897 [PubMed: 25501036]

Bennett C, Gale SD, Garrett ME, Newton ML, Callaway EM, Murphy GJ, & Olsen SR (2019). Higher-order thalamic circuits channel parallel streams of visual information in mice. Neuron, 102(2), 477–492.e5. 10.1016/j.neuron.2019.02.010 [PubMed: 30850257]

Bickford ME, Zhou N, Krahe TE, Govindaiah G, & Guido W (2015). Retinal and tectal "driver-like" inputs converge in the shell of the mouse dorsal lateral geniculate nucleus. Journal of Neuroscience, 35(29), 10523–10534. 10.1523/JNEUROSCI.3375-14.2015 [PubMed: 26203147]

Binkofski F, Seitz RJ, Arnold S, Classen J, Benecke R, & Freund HJ (1996). Thalamic metbolism and corticospinal tract integrity determine motor recovery in stroke. Annals of Neurology, 39(4), 460–470. 10.1002/ana.410390408 [PubMed: 8619524]

Bosch-Bouju C, Hyland BI, & Parr-Brownlie LC (2013). Motor thalamus integration of cortical, cerebellar and basal ganglia information: Implications for normal and parkinsonian conditions. Frontiers in Computational Neuroscience, 7, 163. 10.3389/fncom.2013.00163 [PubMed: 24273509]

Böttcher C, Schlickeiser S, Sneeboer MAM, Kunkel D, Knop A, Paza E, Fidzinski P, Kraus L, Snijders GJL, Kahn RS, Schulz AR, Mei HE, NBB-Psy Hol EM, Siegmund B, Glauben R, Spruth EJ, de Witte LD, & Priller J (2019). Human microglia regional heterogeneity and phenotypes determined by multiplexed single-cell mass cytometry. Nature Neuroscience, 22(1), 78–90. 10.1038/s41593-018-0290-2 [PubMed: 30559476]

Campbell PW, Govindaiah G, Masterson SP, Bickford ME, & Guido W (2020). Synaptic properties of the feedback connections from the thalamic reticular nucleus to the dorsal lateral geniculate nucleus. Journal of Neurophysiology, 124(2), 404–417. 10.1152/jn.00757.2019 [PubMed: 32609582]

Cao Z, Harvey SS, Bliss TM, Cheng MY, & Steinberg GK (2020). Inflammatory responses in the secondary thalamic injury after cortical ischemic stroke. Frontiers in Neurology, 11, 236. 10.3389/fneur.2020.00236 [PubMed: 32318016]

Centers for Disease Control and Prevention. (2015). Stroke facts www.cdc.gov/stroke/facts.htm

Clemente-Perez A, Makinson SR, Higashikubo B, Brovarney S, Cho FS, Urry A, Holden SS, Wimer M, Dávid C, Fenno LE, Acsády L, Deisseroth K, & Paz JT (2017). Distinct thalamic reticular cell types differentially modulate normal and pathological cortical rhythms. Cell Reports, 19(10), 2130–2142. 10.1016/j.celrep.2017.05.044 [PubMed: 28591583]

Collins DP, Anastasiades PG, Marlin JJ, & Carter AG (2018). Reciprocal circuits linking the prefrontal cortex with dorsal and ventral thalamic nuclei. Neuron, 98(2), 366–379.e4. 10.1016/j.neuron.2018.03.024 [PubMed: 29628187]

Cornwall J, Cooper JD, & Phillipson OT (1990). Projections to the rostral reticular thalamic nucleus in the rat. Experimental Brain Research, 80(1), 157–171. 10.1007/BF00228857 [PubMed: 2358025]

Crabtree JW (1992). The somatotopic organization within the cat's thalamic reticular nucleus. European Journal of Neuroscience, 4(12), 1352–1361. 10.1111/j.1460-9568.1992.tb00160.x

Crabtree JW (2018). Functional diversity of thalamic reticular subnet-works. Frontiers in Systems Neuroscience, 12, 41. 10.3389/fnsys.2018.00041 [PubMed: 30405364]

Dean PJA, & Sterr A (2013). Long-term effects of mild traumatic brain injury on cognitive performance. Frontiers in Human Neuroscience, 7, 30. 10.3389/fnhum.2013.00030 [PubMed: 23408228]

Dewan MC, Rattani A, Gupta S, Baticulon RE, Hung Y-C, Punchak M, Agrawal A, Adeleye AO, Shrime MG, Rubiano AM, Rosenfeld JV, & Park KB (2018). Estimating the global incidence of traumatic brain injury. Journal of Neurosurgery, 130(4), 1080–1097. 10.3171/2017.10.JNS17352

Dickerson MR, Bailey ZS, Murphy SF, Urban MJ, & VandeVord PJ (2020). Glial activation in the thalamus contributes to vestibulomotor deficits following blast-induced neurotrauma. Frontiers in Neurology, 11, 618. 10.3389/fneur.2020.00618 [PubMed: 32760340]

Escartin C, Galea E, Lakatos A, O'Callaghan JP, Petzold GC, Serrano-Pozo A, Steinhäuser C, Volterra A, Carmignoto G, Agarwal A, Allen NJ, Araque A, Barbeito L, Barzilai A, Bergles DE, Bonvento G, Butt AM, Chen W-T, Cohen-Salmon M, ..., Verkhratsky A (2021). Reactive astrocyte nomenclature, definitions, and future directions. Nature Neuroscience, 24(3), 312–325. 10.1038/s41593-020-00783-4 [PubMed: 33589835]

Fama R, & Sullivan EV (2015). Thalamic structures and associated cognitive functions: Relations with age and aging. Neuroscience and Biobehavioral Reviews, 54, 29–37. 10.1016/j.neubiorev.2015.03.008 [PubMed: 25862940]

Ferguson PL, Smith GM, Wannamaker BB, Thurman DJ, Pickelsimer EE, & Selassie AW (2010). A population-based study of risk of epilepsy after hospitalization for traumatic brain injury. Epilepsia, 51(5), 891–898. 10.1111/j.1528-1167.2009.02384.x [PubMed: 19845734]

Floyd CL, Golden KM, Black RT, Hamm RJ, & Lyeth BG (2002). Craniectomy position affects Morris water maze performance and hippocampal cell loss after parasagittal fluid percussion. Journal of Neurotrauma, 19(3), 303–316. 10.1089/089771502753594873 [PubMed: 11939498]

Fraser DA, Pisalyaput K, & Tenner AJ (2010). C1q enhances microglial clearance of apoptotic neurons and neuronal blebs, and modulates subsequent inflammatory cytokine production. Journal of Neurochemistry, 112(3), 733–743. 10.1111/j.1471-4159.2009.06494.x [PubMed: 19919576]

Gauthier J, Meijer IA, Lessel D, Mencacci NE, Krainc D, Hempel M, Tsiakas K, Prokisch H, Rossignol E, Helm MH, Rodan LH, Karamchandani J, Carecchio M, Lubbe SJ, Telegrafi A, Henderson LB, Lorenzo K, Wallace SE, Glass IA, ..., Campeau PM (2018). Recessive mutations in VPS13D cause childhood onset movement disorders. Annals of Neurology, 83(6), 1089–1095. 10.1002/ana.25204 [PubMed: 29518281]

Gentet LJ, & Ulrich D (2003). Strong, reliable and precise synaptic connections between thalamic relay cells and neurones of the nucleus reticularis in juvenile rats. Journal of Physiology, 546(Pt 3), 801–811. 10.1113/jphysiol.2002.032730

Grossman EJ, Ge Y, Jensen JH, Babb JS, Miles L, Reaume J, Silver JM, Grossman RI, & Inglese M (2012). Thalamus and cognitive impairment in mild traumatic brain injury: A diffusional kurtosis imaging study. Journal of Neurotrauma, 29(13), 2318–2327. 10.1089/neu.2011.1763 [PubMed: 21639753]

Grossman EJ, & Inglese M (2016). The role of thalamic damage in mild traumatic brain injury. Journal of Neurotrauma, 33(2), 163–167. 10.1089/neu.2015.3965 [PubMed: 26054745]

Guillery RW (1995). Anatomical evidence concerning the role of the thalamus in corticocortical communication: A brief review. Journal of Anatomy, 187(Pt 3), 583–592. [PubMed: 8586557]

Gulcebi MI, Ketenci S, Linke R, Hacıoğlu H, Yanalı H, Veliskova J, Moshé SL, Onat F, & Çavdar S (2012). Topographical connections of the substantia nigra pars reticulata to higher-order thalamic nuclei in the rat. Brain Research Bulletin, 87(2), 312–318. 10.1016/j.brainresbull.2011.11.005 [PubMed: 22108631]

Halassa MM, & Acsády L (2016). Thalamic inhibition: Diverse sources, diverse scales. Trends in Neurosciences, 39(10), 680–693. 10.1016/j.tins.2016.08.001 [PubMed: 27589879]

Hazra A, Corbett BF, You JC, Aschmies S, Zhao L, Li K, Lepore AC, Marsh ED, & Chin J (2016). Corticothalamic network dysfunction and behavioral deficits in a mouse model of Alzheimer's disease. Neurobiology of Aging, 44, 96–107. 10.1016/j.neurobiolaging.2016.04.016 [PubMed: 27318137]

Hazra A, Macolino C, Elliott MB, & Chin J (2014). Delayed thalamic astrocytosis and disrupted sleep-wake patterns in a preclinical model of traumatic brain injury. Journal of Neuroscience Research, 92(11), 1434–1445. 10.1002/jnr.23430 [PubMed: 24964253]

Hochstenbach JB, den Otter R, & Mulder TW (2003). Cognitive recovery after stroke: A 2-year follow-up. Archives of Physical Medicine and Rehabilitation, 84(10), 1499–1504. 10.1016/S0003-9993(03)00370-8 [PubMed: 14586918]

Hoerder-Suabedissen A, Hayashi S, Upton L, Nolan Z, Casas-Torremocha D, Grant E, Viswanathan S, Kanold PO, Clasca F, Kim Y, & Molnár Z (2018). Subset of cortical layer 6b neurons selectively innervates higher order thalamic nuclei in mice. Cerebral Cortex, 28(5), 1882–1897. 10.1093/cercor/bhy036 [PubMed: 29481606]

Hol EM, & Pekny M (2015). Glial fibrillary acidic protein (GFAP) and the astrocyte intermediate filament system in diseases of the central nervous system. Current Opinion in Cell Biology, 32, 121–130. 10.1016/j.ceb.2015.02.004 [PubMed: 25726916]

Holden SS, Grandi FC, Aboubakr O, Higashikubo B, Cho FS, Chang AH, & Paz JT (2021). Complement factor C1q mediates sleep spindle loss and epileptic spikes after mild brain injury. Science, 373(6560). 10.112/science.abj2685

Hopperton KE, Mohammad D, Trépanier MO, Giuliano V, & Bazinet RP (2018). Markers of microglia in post-mortem brain samples from patients with Alzheimer's disease: A systematic review. Molecular Psychiatry, 23(2), 177–198. 10.1038/mp.2017.246 [PubMed: 29230021]

Hoseini MS, Higashikubo B, Cho FS, Chang AH, Clemente-Perez A, Lew I, Ciesielska A, Stryker MP, & Paz JT (2021). Gamma rhythms and visual information in mouse V1 specifically modulated by somatostatin+ neurons in reticular thalamus. eLife, 10, e61437. 10.7554/eLife.61437 [PubMed: 33843585]

Houser CR, Vaughn JE, Barber RP, & Roberts E (1980). GABA neurons are the major cell type of the nucleus reticularis thalami. Brain Research, 200(2), 341–354. 10.1016/0006-8993(80)90925-7 [PubMed: 7417821]

Hwang K, Bertolero MA, Liu WB, & D'Esposito M (2017). The human thalamus is an integrative hub for functional brain networks. Journal of Neuroscience, 37(23), 5594–5607. 10.1523/JNEUROSCI.0067-17.2017 [PubMed: 28450543]

Imai Y, Ibata I, Ito D, Ohsawa K, & Kohsaka S (1996). A novel gene iba1 in the major histocompatibility complex class III region encoding an EF hand protein expressed in a monocytic lineage. Biochemical and Biophysical Research Communications, 224(3), 855–862. 10.1006/bbrc.1996.1112 [PubMed: 8713135]

Ito D, Tanaka K, Suzuki S, Dembo T, & Fukuuchi Y (2001). Enhanced expression of iba1, ionized calcium-binding adapter molecule 1, after transient focal cerebral ischemia in rat brain. Stroke, 32(5), 1208–1215. 10.1161/01.STR.32.5.1208 [PubMed: 11340235]

Jourdan C, Azouvi P, Genêt F, Selly N, Josseran L, & Schnitzler A (2018). Disability and health consequences of traumatic brain injury: National prevalence. American Journal of Physical Medicine & Rehabilitation, 97(5), 323–331. 10.1097/PHM.0000000000000848 [PubMed: 29016402]

Kessner SS, Eckhard S, Bastian C, Ulrike B, Jens F, Christian G, & Götz T. (2019). Somatosensory deficits after ischemic stroke. Stroke, 50(5), 1116–1123. 10.1161/STROKEAHA.118.023750 [PubMed: 30943883]

Khakh BS, & Sofroniew MV (2015). Diversity of astrocyte functions and phenotypes in neural circuits. Nature Neuroscience, 18(7), 942–952. 10.1038/nn.4043 [PubMed: 26108722]

Kinnunen KM, Greenwood R, Powell JH, Leech R, Hawkins PC, Bonnelle V, Patel MC, Counsell SJ, & Sharp DJ (2011). White matter damage and cognitive impairment after traumatic brain injury. Brain, 134(Pt 2), 449–463. 10.1093/brain/awq347 [PubMed: 21193486]

Kirst C, Skriabine S, Vieites-Prado A, Topilko T, Bertin P, Gerschenfeld G, Verny F, Topilko P, Michalski N, Tessier-Lavigne M, & Renier N (2020). Mapping the fine-scale organization and plasticity of the brain vasculature. Cell, 180(4), 780–795.e25. 10.1016/j.cell.2020.01.028 [PubMed: 32059781]

Kuchcinski G, Munsch F, Lopes R, Bigourdan A, Su J, Sagnier S, Renou P, Pruvo J-P, Rutt BK, Dousset V, Sibon I, & Tourdias T (2017). Thalamic alterations remote to infarct appear as focal

iron accumulation and impact clinical outcome. Brain, 140(7), 1932–1946. 10.1093/brain/awx114 [PubMed: 28549087]

Lam Y-W, & Sherman SM (2011). Functional organization of the thalamic input to the thalamic reticular nucleus. Journal of Neuroscience, 31(18), 6791–6799. 10.1523/JNEUROSCI.3073-10.2011 [PubMed: 21543609]

Langen K-J, Salber D, Hamacher K, Stoffels G, Reifenberger G, Pauleit D, Coenen HH, & Zilles K (2007). Detection of secondary thalamic degeneration after cortical infarction using cis-4–18F-fluoro-D-proline. Journal of Nuclear Medicine, 48(9), 1482–1491. 10.2967/jnumed.107.041699 [PubMed: 17704244]

Lee CC (2013). Thalamic and cortical pathways supporting auditory processing. Brain and Language, 126(1), 22–28. 10.1016/j.bandl.2012.05.004 [PubMed: 22728130]

Lee J-H, Latchoumane C-FV, Park J, Kim J, Jeong J, Lee K-H, & Shin H-S (2019). The rostroventral part of the thalamic reticular nucleus modulates fear extinction. Nature Communications, 10(1), 4637. 10.1038/s41467-019-12496-9

Liddelow SA, Guttenplan KA, Clarke LE, Bennett FC, Bohlen CJ, Schirmer L, Bennett ML, Münch AE, Chung W-S, Peterson TC, Wilton DK, Frouin A, Napier BA, Panicker N, Kumar M, Buckwalter MS, Rowitch DH, Dawson VL, Dawson TM, ..., Barres BA (2017). Neurotoxic reactive astrocytes are induced by activated microglia. Nature, 541(7638), 481–487. 10.1038/nature21029 [PubMed: 28099414]

Liepert J, Restemeyer C, Kucinski T, Zittel S, & Weiller C (2005). Motor strokes: The lesion location determines motor excitability changes. Stroke, 36(12), 2648–2653. 10.1161/01.STR.0000189629.10603.02 [PubMed: 16269647]

Lifshitz J, Kelley BJ, & Povlishock JT (2007). Perisomatic thalamic axotomy after diffuse traumatic brain injury is associated with atrophy rather than cell death. Journal of Neuropathology & Experimental Neurology, 66(3), 218–229. 10.1097/01.jnen.0000248558.75950.4d [PubMed: 17356383]

Lindsay MP, Norrving B, Sacco RL, Brainin M, Hacke W, Martins S, Pandian J, & Feigin V (2019). World Stroke Organization (WSO): Global stroke fact sheet 2019. International Journal of Stroke, 14(8), 806–817. 10.1177/1747493019881353 [PubMed: 31658892]

Lindsay NM, Knutsen PM, Lozada AF, Gibbs D, Karten HJ, & Kleinfeld D (2019). Orofacial movements involve parallel corticobulbar projections from motor cortex to trigeminal premotor nuclei. Neuron, 104(4), 765–780.e3. 10.1016/j.neuron.2019.08.032 [PubMed: 31587918]

Loane DJ, Kumar A, Stoica BA, Cabatbat R, & Faden AI (2014). Progressive neurodegeneration after experimental brain trauma: Association with chronic microglial activation. Journal of Neuropathology and Experimental Neurology, 73(1), 14–29. 10.1097/NEN.0000000000000021 [PubMed: 24335533]

Lozsádi DA (1994). Organization of cortical afferents to the rostral, limbic sector of the rat thalamic reticular nucleus. Journal of Comparative Neurology, 341(4), 520–533. 10.1002/cne.903410408

Lutkenhoff ES, Wright MJ, Shrestha V, Real C, McArthur DL, Buitrago-Blanco M, Vespa PM, & Monti MM (2020). The subcortical basis of outcome and cognitive impairment in TBI: A longitudinal cohort study. Neurology, 95(17), e2398–e2408. 10.1212/WNL.0000000000010825 [PubMed: 32907958]

Makinson CD, Tanaka BS, Sorokin JM, Wong JC, Christian CA, Goldin AL, Escayg A, & Huguenard JR (2017). Regulation of thalamic and cortical network synchrony by Scn8a. Neuron, 93(5), 1165–1179.e6. 10.1016/j.neuron.2017.01.031 [PubMed: 28238546]

Manninen E, Chary K, Lapinlampi N, Andrade P, Paananen T, Sierra A, Tohka J, Gröhn O, & Pitkänen A (2021). Acute thalamic damage as a prognostic biomarker for post-traumatic epileptogenesis. Epilepsia 10.1111/epi.16986

Masuda T, Sankowski R, Staszewski O, & Prinz M (2020). Microglia heterogeneity in the single-cell era. Cell Reports, 30(5), 1271–1281. 10.1016/j.celrep.2020.01.010 [PubMed: 32023447]

Matias I, Morgado J, & Gomes FCA (2019). Astrocyte heterogeneity: Impact to brain aging and disease. Frontiers in Aging Neuroscience, 11, 59. 10.3389/fnagi.2019.00059 [PubMed: 30941031]

McCormick DA, & Bal T (1997). Sleep and arousal: Thalamocortical mechanisms. Annual Review of Neuroscience, 20, 185–215. 10.1146/annurev.neuro.20.1.185

Mitchell AS (2015). The mediodorsal thalamus as a higher order thalamic relay nucleus important for learning and decision-making. Neuroscience & Biobehavioral Reviews, 54, 76–88. 10.1016/j.neubiorev.2015.03.001 [PubMed: 25757689]

Monavarfeshani A, Sabbagh U, & Fox MA (2017). Not a one-trick pony: Diverse connectivity and functions of the rodent lateral geniculate complex. Visual Neuroscience, 34, E012. 10.1017/S0952523817000098 [PubMed: 28965517]

Müller A, Stellmacher A, Freitag CE, Landgraf P, & Dieterich DC (2015). Monitoring astrocytic proteome dynamics by cell type-specific protein labeling. PLoS One, 10(12), e0145451. 10.1371/journal.pone.0145451 [PubMed: 26690742]

Nakajima M, & Halassa MM (2017). Thalamic control of functional cortical connectivity. Current Opinion in Neurobiology, 44, 127–131. 10.1016/j.conb.2017.04.001 [PubMed: 28486176]

Nascimento LR, Scianni AA, Ada L, Fantauzzi MO, Hirochi TL, & Teixeira-Salmela LF (2021). Predictors of return to work after stroke: A prospective, observational cohort study with 6 months follow-up. Disability and Rehabilitation, 43(4), 525–529. 10.1080/09638288.2019.1631396 [PubMed: 31242399]

Ohara T, Yamamoto Y, Tamura A, Ishii R, & Murai T (2010). The infarct location predicts progressive motor deficits in patients with acute lacunar infarction in the lenticulostriate artery territory. Journal of the Neurological Sciences, 293(1), 87–91. 10.1016/j.jns.2010.02.027 [PubMed: 20334882]

Pappata S, Levasseur M, Gunn RN, Myers R, Crouzel C, Syrota A, Jones T, Kreutzberg GW, & Banati RB (2000). Thalamic microglial activation in ischemic stroke detected in vivo by PET and [11C]PK1195. Neurology, 55(7), 1052–1054. 10.1212/wnl.55.7.1052 [PubMed: 11061271]

Parnaudeau S, Bolkan SS, & Kellendonk C (2018). The mediodorsal thalamus: An essential partner of prefrontal cortex for cognition. Biological Psychiatry, 83(8), 648–656. 10.1016/j.biopsych.2017.11.008 [PubMed: 29275841]

Paxinos G, & Franklin K (2007). The mouse brain in stereotaxic coordinates (3rd ed.). Academic Press.

Paz JT, Bryant AS, Peng K, Fenno L, Yizhar O, Frankel WN, Deis seroth K, & Huguenard JR (2011). A new mode of corticothalamic transmission revealed in the Gria4−/− model of absence epilepsy. Nature Neuroscience, 14(9), 1167–1173. 10.1038/nn.2896 [PubMed: 21857658]

Paz JT, Christian CA, Parada I, Prince DA, & Huguenard JR (2010). Focal cortical infarcts alter intrinsic excitability and synaptic excitation in the reticular thalamic nucleus. Journal of Neuroscience, 30(15), 5465–5479. 10.1523/JNEUROSCI.5083-09.2010 [PubMed: 20392967]

Paz JT, Davidson TJ, Frechette ES, Delord B, Parada I, Peng K, Deisseroth K, & Huguenard JR (2013). Closed-loop optogenetic control of thalamus as a new tool to interrupt seizures after cortical injury. Nature Neuroscience, 16(1), 64–70. 10.1038/nn.3269 [PubMed: 23143518]

Perry BAL, & Mitchell AS (2019). Considering the evidence for anterior and laterodorsal thalamic nuclei as higher order relays to cortex. Frontiers in Molecular Neuroscience, 12, 167. 10.3389/fnmol.2019.00167 [PubMed: 31333412]

Power BD, & Looi JC (2015). The thalamus as a putative biomarker in neurodegenerative disorders. Australian & New Zealand Journal of Psychiatry, 49(6), 502–518. 10.1177/0004867415585857

Puelles L, Martinez-de-la-Torre M, Ferran J-L, & Watson C (2012). Chapter 9—Diencephalon. In Watson C, Paxinos G, & Puelles L (Eds.), The mouse nervous system (pp. 313–336). Academic Press.

Ramcharan EJ, Gnadt JW, & Sherman SM (2005). Higher-order thalamic relays burst more than first-order relays. Proceedings of the National Academy of Sciences, 102(34), 12236–12241. 10.1073/pnas.0502843102

Ramlackhansingh AF, Brooks DJ, Greenwood RJ, Bose SK, Turkheimer FE, Kinnunen KM, Gentleman S, Heckemann RA, Gunanayagam K, Gelosa G, & Sharp DJ (2011). Inflammation after trauma: Microglial activation and traumatic brain injury. Annals of Neurology, 70(3), 374–383. 10.1002/ana.22455 [PubMed: 21710619]

Reinhold K, Lien AD, & Scanziani M (2015). Distinct recurrent versus afferent dynamics in cortical visual processing. Nature Neuroscience, 18(12), 1789–1797. 10.1038/nn.4153 [PubMed: 26502263]

Ritter-Makinson S, Clemente-Perez A, Higashikubo B, Cho FS, Holden SS, Bennett E, Chkhaidze A, Eelkman Rooda OHJ, Cornet M-C, Hoebeek FE, Yamakawa K, Cilio MR, Delord B, & Paz JT (2019). Augmented reticular thalamic bursting and seizures in Scn1a-Dravet syndrome. Cell Reports, 26(1), 54–64.e6. 10.1016/j.celrep.2018.12.018 [PubMed: 30605686]

Rosa JM, Farre-Alins V, Ortega MC, Navarrete M, Lopez-Rodriguez AB, Palomino-Antolin A, Fernandez-Lopez E, Vila-Del Sol V, Decouty C, Narros-Fernandez P, Clemente D, & Egea J (2021). TLR4-pathway impairs synaptic number and cerebrovascular functions through astrocyte activation following traumatic brain injury. British Journal of Pharmacology 10.1111/bph.15488

Rose CR, & Kirchhoff F (2015). Glial heterogeneity: The increasing complexity of the brain. e-Neuroforum, 6(3), 59–62. 10.1007/s13295-015-0012-0

Rosenberg MF, & Molofsky AV (2020). Location, location, location: Transcriptional control of astrocyte heterogeneity. Trends in Immunology, 41(9), 753–755. 10.1016/j.it.2020.07.011 [PubMed: 32800455]

Ross DT, & Ebner FF (1990). Thalamic retrograde degeneration following cortical injury: An excitotoxic process? Neuroscience, 35(3), 525–550. 10.1016/0306-4522(90)90327-z [PubMed: 2166245]

Sandsmark DK, Elliott JE, & Lim MM (2017). Sleep-wake disturbances after traumatic brain injury: Synthesis of human and animal studies. Sleep 10.1093/sleep/zsx044

Schaechter JD (2004). Motor rehabilitation and brain plasticity after hemiparetic stroke. Progress in Neurobiology, 73(1), 61–72. 10.1016/j.pneurobio.2004.04.001 [PubMed: 15193779]

Scott DA, Tabarean I, Tang Y, Cartier A, Masliah E, & Roy S (2010). A pathologic cascade leading to synaptic dysfunction in alpha-synuclein-induced neurodegeneration. Journal of Neuroscience, 30(24), 8083–8095. 10.1523/JNEUROSCI.1091-10.2010 [PubMed: 20554859]

Scott G, Hellyer PJ, Ramlackhansingh AF, Brooks DJ, Matthews PM, & Sharp DJ (2015). Thalamic inflammation after brain trauma is associated with thalamo-cortical white matter damage. Journal of Neuroinflammation, 12(1), 224. 10.1186/s12974-015-0445-y [PubMed: 26627199]

Shapiro LA, Perez ZD, Foresti ML, Arisi GM, & Ribak CE (2009). Morphological and ultrastructural features of Iba1-immunolabeled microglial cells in the hippocampal dentate gyrus. Brain Research, 1266, 29–36. 10.1016/j.brainres.2009.02.031 [PubMed: 19249294]

Sherman SM (2007). The thalamus is more than just a relay. Current Opinion in Neurobiology, 17(4), 417–422. 10.1016/j.conb.2007.07.003 [PubMed: 17707635]

Sherman SM (2016). Thalamus plays a central role in ongoing cortical functioning. Nature Neuroscience, 19(4), 533–541. 10.1038/nn.4269 [PubMed: 27021938]

Sherman SM, & Guillery RW (1996). Functional organization of thalamocortical relays. Journal of Neurophysiology, 76(3), 1367–1395. 10.1152/jn.1996.76.3.1367 [PubMed: 8890259]

Sherman SM, & Guillery RW (2002). The role of the thalamus in the flow of information to the cortex. Philosophical Transactions of the Royal Society of London. Series B, Biological Sciences, 357(1428), 1695–1708. 10.1098/rstb.2002.1161 [PubMed: 12626004]

Sherman SM, & Guillery RW (2006). Exploring the thalamus and its role in cortical function (2nd ed., p. xxi, 484). MIT Press.

Sherman SM, & Guillery RW (2013). Functional Connections of Cortical Areas: A New View from the Thalamus MIT Press.

Sherman SM, & Koch C (1986). The control of retinogeniculate transmission in the mammalian lateral geniculate nucleus. Experimental Brain Research, 63(1), 1–20. 10.1007/BF00235642 [PubMed: 3015651]

Sørensen JC, Dalmau I, Zimmer J, & Finsen B (1996). Microglial reactions to retrograde degeneration of tracer-identified thalamic neurons after frontal sensorimotor cortex lesions in adult rats. Experimental Brain Research, 112(2), 203–212. 10.1007/BF00227639 [PubMed: 8951389]

Stocchetti N, & Zanier ER (2016). Chronic impact of traumatic brain injury on outcome and quality of life: A narrative review. Critical Care (London, England), 20(1), 148. 10.1186/s13054-016-1318-1

Suarez-Mier GB, & Buckwalter MS (2015). Glial fibrillary acidic protein-expressing glia in the mouse lung. ASN Neuro, 7(5). 10.1177/1759091415601636

Sul B, Lee KB, Hong BY, Kim JS, Kim J, Hwang WS, & Lim SH (2019). Association of lesion location with long-term recovery in post-stroke aphasia and language deficits. Frontiers in Neurology, 10, 776. 10.3389/fneur.2019.00776 [PubMed: 31396146]

Van Horn SC, & Sherman SM (2007). Fewer driver synapses in higher order than in first order thalamic relays. Neuroscience, 146(1), 463–470. 10.1016/j.neuroscience.2007.01.026 [PubMed: 17320295]

Vantomme G, Osorio-Forero A, Lüthi A, & Fernandez LMJ (2019). Regulation of local sleep by the thalamic reticular nucleus. Frontiers in Neuroscience, 13, 576. 10.3389/fnins.2019.00576 [PubMed: 31231186]

Walker DG, & Lue L-F (2015). Immune phenotypes of microglia in human neurodegenerative disease: Challenges to detecting microglial polarization in human brains. Alzheimer's Research & Therapy, 7(1), 1–9. 10.1186/s13195-015-0139-9

Weishaupt JH, Hyman T, & Dikic I (2016). Common molecular pathways in amyotrophic lateral sclerosis and frontotemporal dementia. Trends in Molecular Medicine, 22(9), 769–783. 10.1016/j.molmed.2016.07.005 [PubMed: 27498188]

Wells MF, Wimmer RD, Schmitt LI, Feng G, & Halassa MM (2016). Thalamic reticular impairment underlies attention deficit in Ptchd1(Y/–) mice. Nature, 532(7597), 58–63. 10.1038/nature17427 [PubMed: 27007844]

Worker CJ, Li W, Feng C-Y, Souza LAC, Gayban AJB, Cooper SG, Afrin S, Romanick S, Ferguson BS, & Feng Earley Y (2020). The neuronal (pro)renin receptor and astrocyte inflammation in the central regulation of blood pressure and blood glucose in mice fed a high-fat diet. American Journal of Physiology-Endocrinology and Metabolism, 318(5), E765–E778. 10.1152/ajpendo.00406.2019 [PubMed: 32228320]

Xin W, & Bonci A (2018). Functional astrocyte heterogeneity and implications for their role in shaping neurotransmission. Frontiers in Cellular Neuroscience, 12, 141. 10.3389/fncel.2018.00141 [PubMed: 29896091]

Yuan P, & Raz N (2014). Prefrontal cortex and executive functions in healthy adults: A meta-analysis of structural neuroimaging studies. Neuroscience and Biobehavioral Reviews, 42, 180–192. 10.1016/j.neubiorev.2014.02.005 [PubMed: 24568942]

Zaloshnja E, Miller T, Langlois JA, & Selassie AW (2008). Prevalence of long-term disability from traumatic brain injury in the civilian population of the United States, 2005. Journal of Head Trauma Rehabilitation, 23(6), 394–400. 10.1097/01.HTR.0000341435.52004.ac

Zhang D, Hu X, Qian L, O'Callaghan JP, & Hong J-S (2010). Astrogliosis in CNS pathologies: Is there a role for microglia? Molecular Neurobiology, 41(2–3), 232–241. 10.1007/s12035-010-8098-4 [PubMed: 20148316]

Zikopoulos B, & Barbas H (2006). Prefrontal projections to the thalamic reticular nucleus form a unique circuit for attentional mechanisms. Journal of Neuroscience, 26(28), 7348–7361. 10.1523/JNEUROSCI.5511-05.2006 [PubMed: 16837581]

Zikopoulos B, & Barbas H (2012). Pathways for emotions and attention converge on the thalamic reticular nucleus in primates. Journal of Neuroscience, 32(15), 5338–5350. 10.1523/JNEUROSCI.4793-11.2012 [PubMed: 22496579]

Zimmerman EC, & Grace AA (2018). Prefrontal cortex modulates firing pattern in the nucleus reuniens of the midline thalamus via distinct corticothalamic pathways. European Journal of Neuroscience, 48(10), 3255–3272. 10.1111/ejn.14111

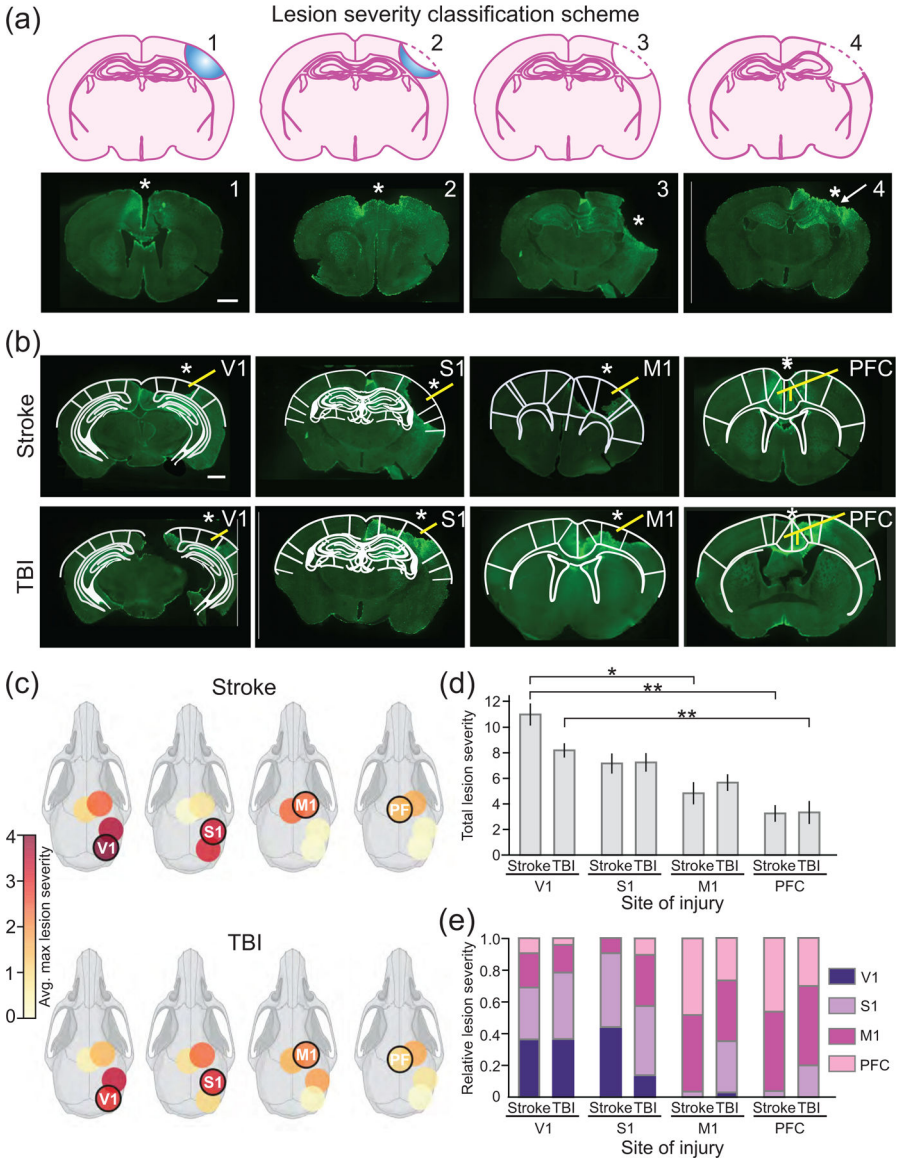


**FIGURE 1.**

Severity of cortical injury by injury site 1 week after cortical stroke or TBI. (a) (top) Schematics of cortical lesion severity as categorized on an index scale from 0 to 4. 0: no cortical inflammation or cavity; 1: cortical inflammation (blue) but no cavity; 2: cortical inflammation and partial cavity; 3: cortical inflammation, loss of the entire cortical column at the lesion site, and near complete or complete cortical loss; and 4: damaged subcortical hippocampus in addition to the cortex. (bottom) Representative images of cortical lesion severity 1–4. From left to right, images are derived from PFC stroke, PFC stroke, S1 stroke, and S1 TBI animals. Arrow in the image of lesion severity 4 indicates a hypertrophic hippocampus. White asterisks indicate the lesion site. Scale bar: 1 mm. (b) Representative low magnification coronal brain sections 1 week following injury at each site, overlaid with the atlas. PFC TBI is bilateral but occasionally impacts one hemisphere more than the other. White asterisks indicate the lesion site. Lesion severity in stroke is as follows, from left to

right: 4,3,4,1. Lesion severity in TBI is as follows, from left to right: 3,4,2,1. Scale bar: 1 mm. (c) Anatomical heatmap indicating position of the impactor (bolded circle) and lesion severity (color) in various cortical sites. Lesion severity is based on the index scale in (a) and represents average maximum lesion severity. $n = 5–8$ mice per targeted injury site. Created with BioRender.com. (d) Total lesion severity in the cortex, consisting of summed lesion severity for each cortical injury site within each injury condition. Bars represent mean maximum injury + SEM. Significant differences in total lesion severity were calculated via the Kruskal–Wallis test with $\alpha = 0.05$ and Dunn's multiple comparison test (*$p < .05$, **$p < .01$). Twelve total comparisons were made (six per injury type). No significant difference was found between each stroke/TBI pair. $n = 5–8$ mice per targeted injury site. (e) Relative lesion severity in each cortical region, normalized to 1. For more detail on how the baseline fluorescence was measured for the bilateral injury in PFC, see Figure 2. Sham mice had no lesions and no significant thalamic inflammation (Figure 3)

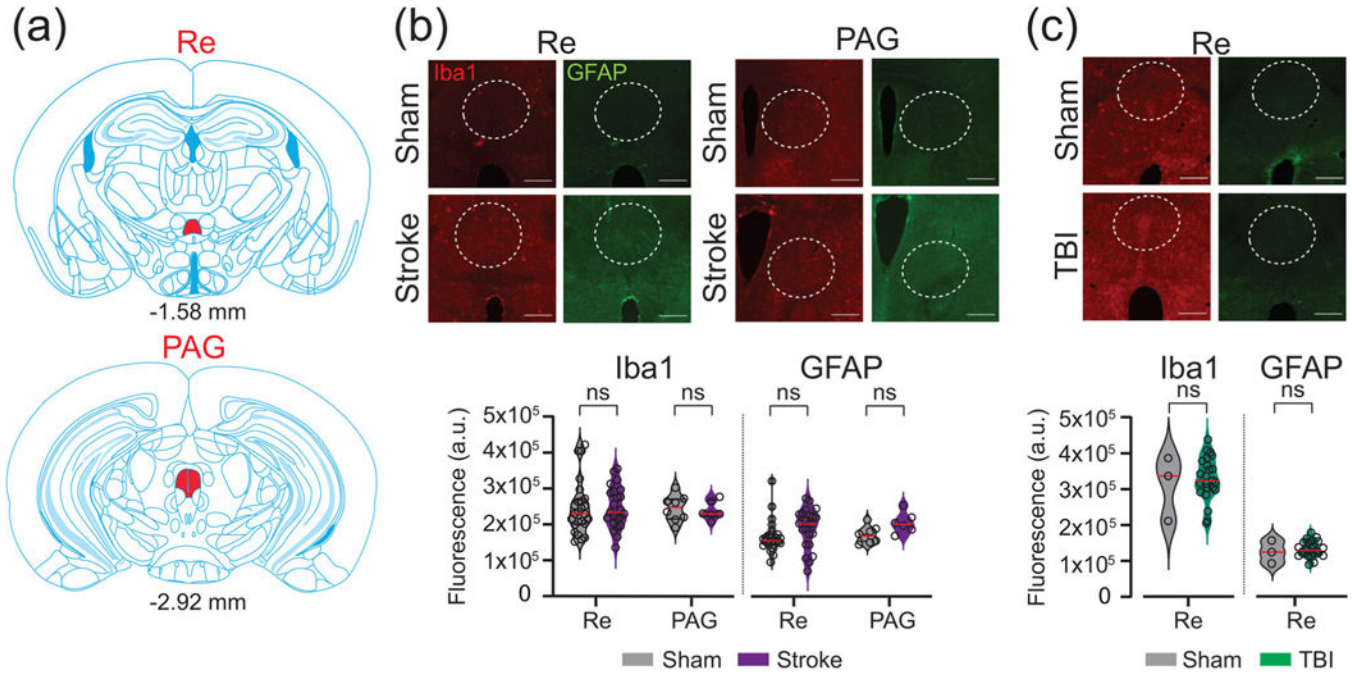


**FIGURE 2.**

Iba1 and GFAP immunofluorescence in reuniens and periaqueductal gray nuclei was used to determine baseline fluorescence for a bilateral injury in the prefrontal cortex. (a) Images indicating in red the approximate position of the nucleus reuniens (Re) or the approximate position of the periaqueductal gray nucleus (PAG) used as baseline controls for injury to the PFC, given the bilateral nature of the injury and the inapplicability of the contralateral hemisphere as an appropriate control. Bregma coordinates of atlas images are indicated. (b and c) (top) Representative images of Iba1 and GFAP labeling indicating the approximate location of the regions analyzed from a stroke (b) and a TBI mouse (c). Scale bar: 200 $\mu$m. (bottom) Violin plots showing the quantification of Iba1 and GFAP immunofluorescence in the Re and PAG. No sections were analyzed for PAG in the TBI condition because of the low number of sections containing PAG. Significance was assessed by Mann–Whitney tests using $\alpha = 0.05$ and multiply corrected by the Holm–Sidak method (*$p < .05$, **$p < .01$, ns $p > .05$). $n = 3$ ROIs sham TBI, all other groups $n = 25$

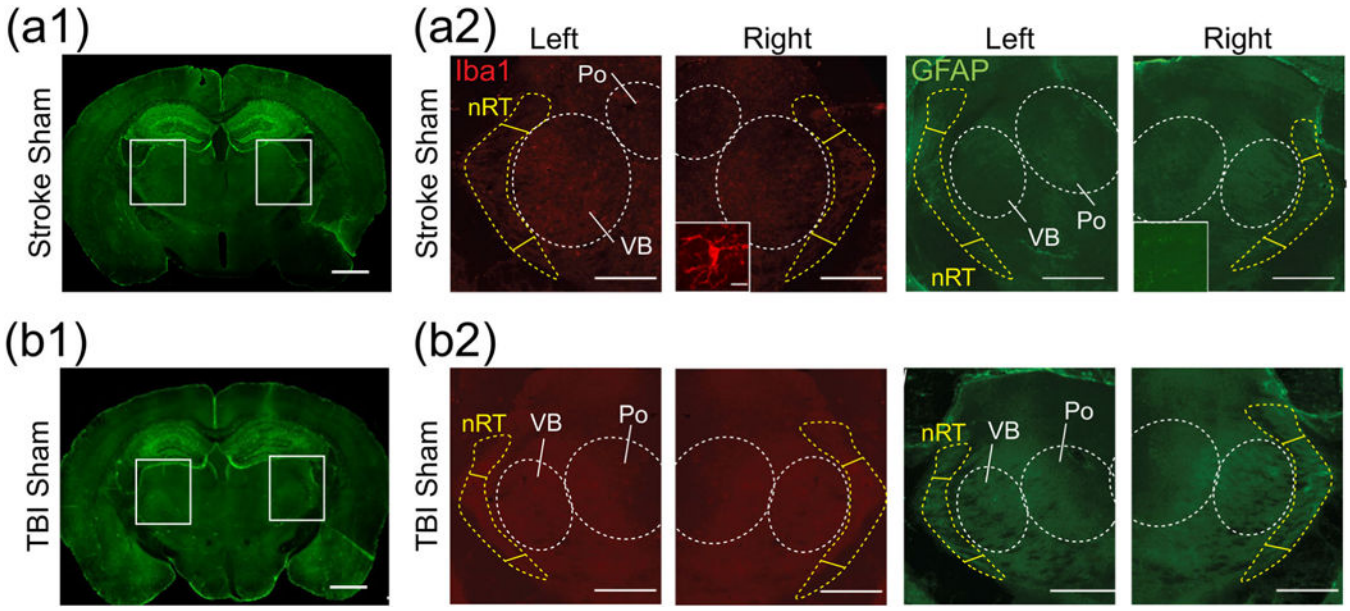


**FIGURE 3.**

Sham mice do not exhibit cortical injury or significant micro- or astrogliosis in either hemisphere. (a1 and b1) Representative low magnification coronal brain sections from a stroke sham (a1) and a TBI sham (b1) mouse. White squares indicate the approximate regions from which close-up images were obtained and analyzed. Scale bar: 1 mm. (a2 and b2) Representative close-up images of both Iba1 and GFAP-labeled brain sections from sham stroke (a2) and sham TBI (b2) mice with relevant regions of interest demarcated. Images are acquired from both the left and right hemispheres from the regions indicated in (a1 and b1). The GABAergic nRT is traced in yellow to distinguish it from the glutamatergic thalamocortical nuclei (white). Insets are high magnification of Iba1 or GFAP labeling. Note the complete lack of GFAP-positive astrocytes in the sham thalamus. Scale bars: 300 $\mu$m, 10 $\mu$m insets

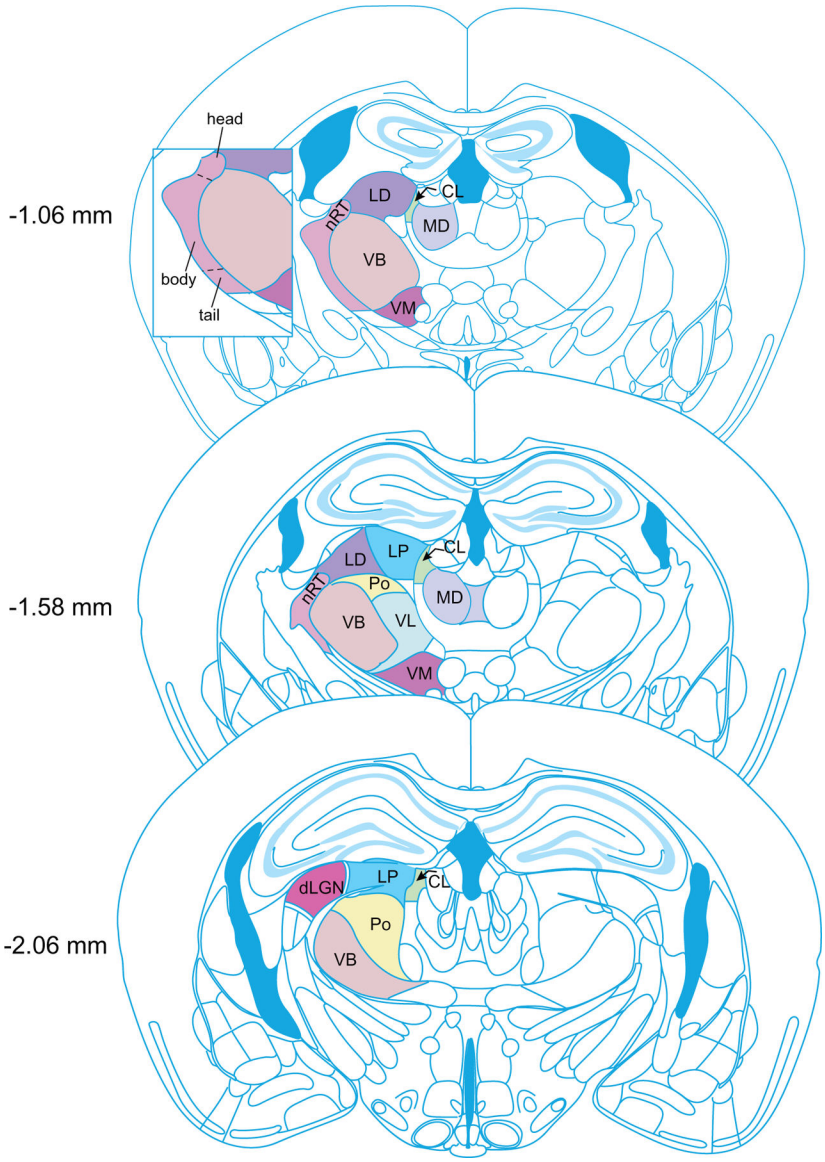


**FIGURE 4.**

Thalamic nuclei assessed for secondary inflammation. Atlas images at different locations (bregma indicated on left), representing the approximate anterior-posterior coordinate of coronal brain sections analyzed for Iba1- and GFAP immunolabeling

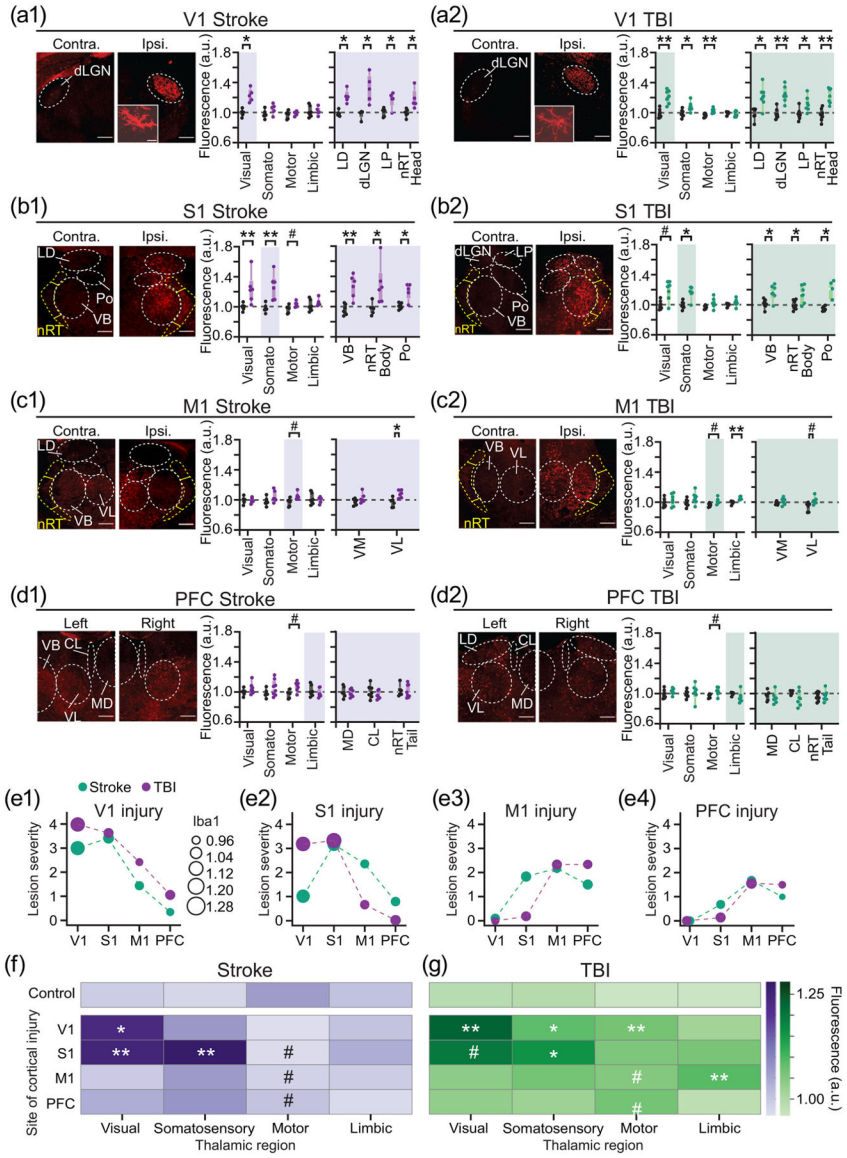


**FIGURE 5.**

Microgliosis in the thalamus following stroke or TBI in different cortical sites mirrors functional corticothalamic connectivity. (a1, b1, c1, and d1) Microgliosis in the visual, somatosensory, motor, and limbic thalamic regions of the thalami after cortical stroke, assessed by raw integrated pixel density taken as a ratio of ipsilateral to contralateral. Note that because of the midline injury to the PFC, the images are designated as corresponding to the left and right hemispheres rather than ipsilateral and contralateral. (rightmost graph) ROI-specific Iba1, a proxy for microgliosis, by corresponding thalamic region. The nRT is indicated in yellow. Inset is a high magnification image of a Iba1-stained microglial cell and is representative of a1–d1. Significance was assessed by Mann–Whitney tests using $\alpha = 0.05$ and multiply corrected by the Holm–Sidak method (*$p < .05$, **$p < .01$, $^{\#}p <$ .05 without multiple comparison correction). Data are represented by Tukey boxplots with whiskers extending to 1.5*IQR from the first and third quartiles. Scale bars: 300 $\mu$m, 10

$\mu$m inset. $n$ = 5–8 mice per targeted injury site. Sham mice had no lesion and no significant thalamic inflammation (see Figure 3). Lesion severities are as follows, from top to bottom, and are representative for thalamic inflammation: 4,3,4,0. (a2–d2) Microgliosis in the visual, somatosensory, motor, and limbic thalamic regions after cortical TBI. Apart from injury type, all other figure parameters in (a1–d1) apply. Inset is a high magnification image of a Iba1-stained microglial cell and is representative of a2–d2. Lesion severities are as follows, from top to bottom, and are representative for thalamic inflammation: 3,3,3,1. (e1–e4) Bubble plots representing average maximum lesion severity in the cortex (y axis) and average inflammation in the corresponding thalamocortical nuclei (bubble size represents Iba1 fluorescence in thalamus). Each panel heading represents the site at which cortical injury was induced, while the x-axis indicates the cortical regions at which lesion severity was analyzed. For instance, (e1) shows that V1 stroke leads to: size 4 lesion in the V1 cortex itself, size 1 lesion in PFC (meaning mild inflammation with no cavity), Iba 1 fluorescence of 1.12 a.u. in visual thalamocortical nuclei (averaged LD, dLGN, and LP), and Iba 1 fluorescence of 1 (meaning no inflammation) in PFC-related thalamocortical nuclei (averaged MD and CL). (f) Sham-normalized heatmap summarizing results from (a1–d1). (g) Sham-normalized heatmap summarizing results from (a2–d2)

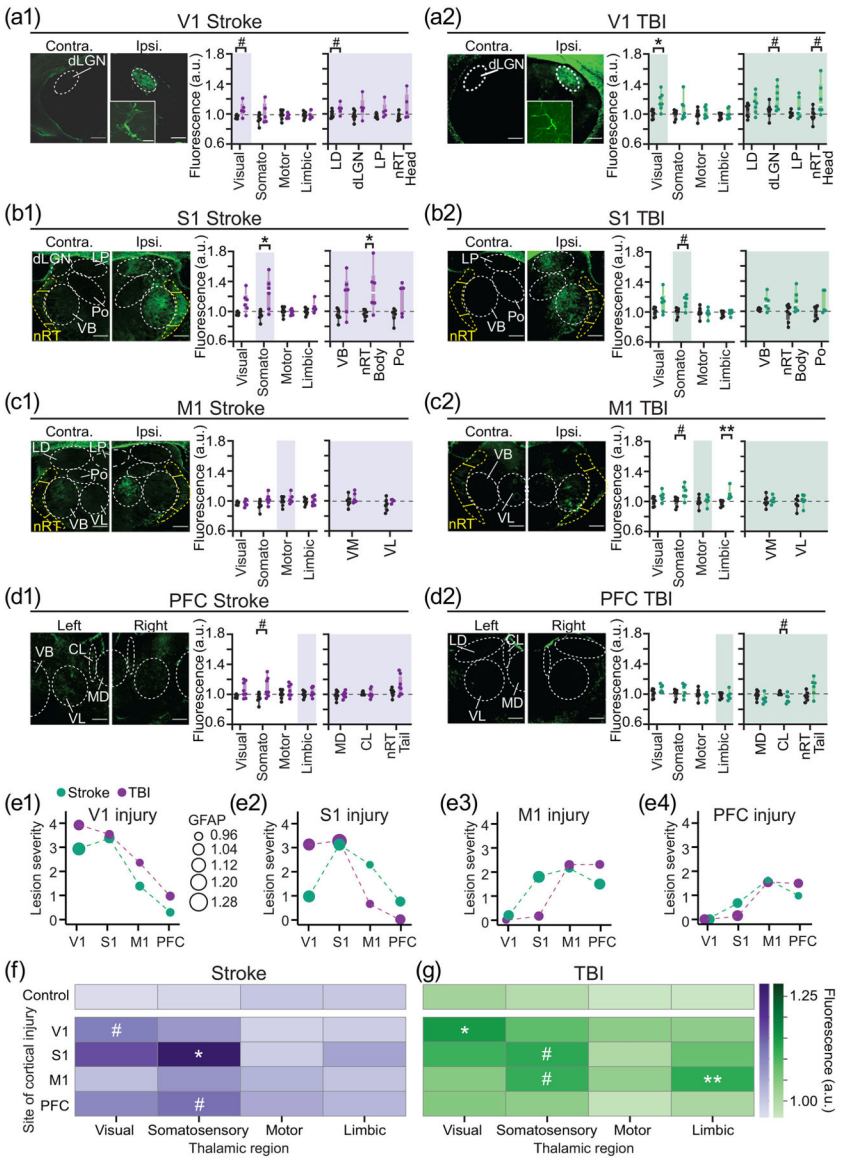


**FIGURE 6.**

Astrogliosis in the thalamus following stroke or TBI in different cortical sites mirrors functional corticothalamic connectivity. (a1, b1, c1, and d1) Astrogliosis in the visual, somatosensory, motor, and limbic thalami after cortical stroke, assessed by raw integrated pixel density taken as a ratio of ipsilateral to contralateral. (rightmost graph) ROI-specific GFAP, a proxy for astrogliosis, by corresponding thalamic region. The nRT is indicated in yellow to designate it as a GABAergic structure. Inset is a high magnification image of a GFAP-stained astrocyte and is representative of a1–d1. Significance was assessed by Mann–Whitney tests using $\alpha = 0.05$ and multiply corrected by the Holm–Sidak method (*$p < .05$, **$p < .01$, $^{\#}p < .05$ without multiple comparison correction). Data are represented by Tukey boxplots with whiskers extending to 1.5*IQR from the first and third quartiles. Scale bars: 300 $\mu$m, 10 $\mu$m inset. $n = 5$–8 mice per targeted injury site. Lesion severities in the region of impact are as follows, from top to bottom: 4,3,0,2. (a2, b2, c2, and d2) Astrogliosis

in the visual, somatosensory, motor, and limbic thalami after cortical TBI. Apart from injury type, all other figure parameters in (a1–d1) also apply. Inset is a high magnification image of a GFAP-stained astrocyte and is representative of a2–d2. Lesion severities in the region of impact are as follows, from top to bottom: 3,4,3,1. (e1–e4) Bubble plots representing average maximum lesion severity in the cortex (y axis) and average inflammation in the corresponding thalamic region (bubble size represents GFAP fluorescence in thalamus). For detailed explanation, please refer to the legend of Figure 5e1–e4. (f) Sham-normalized heatmap summarizing results from (a1–d1). (g) Sham-normalized heatmap summarizing results from (a2–d2)

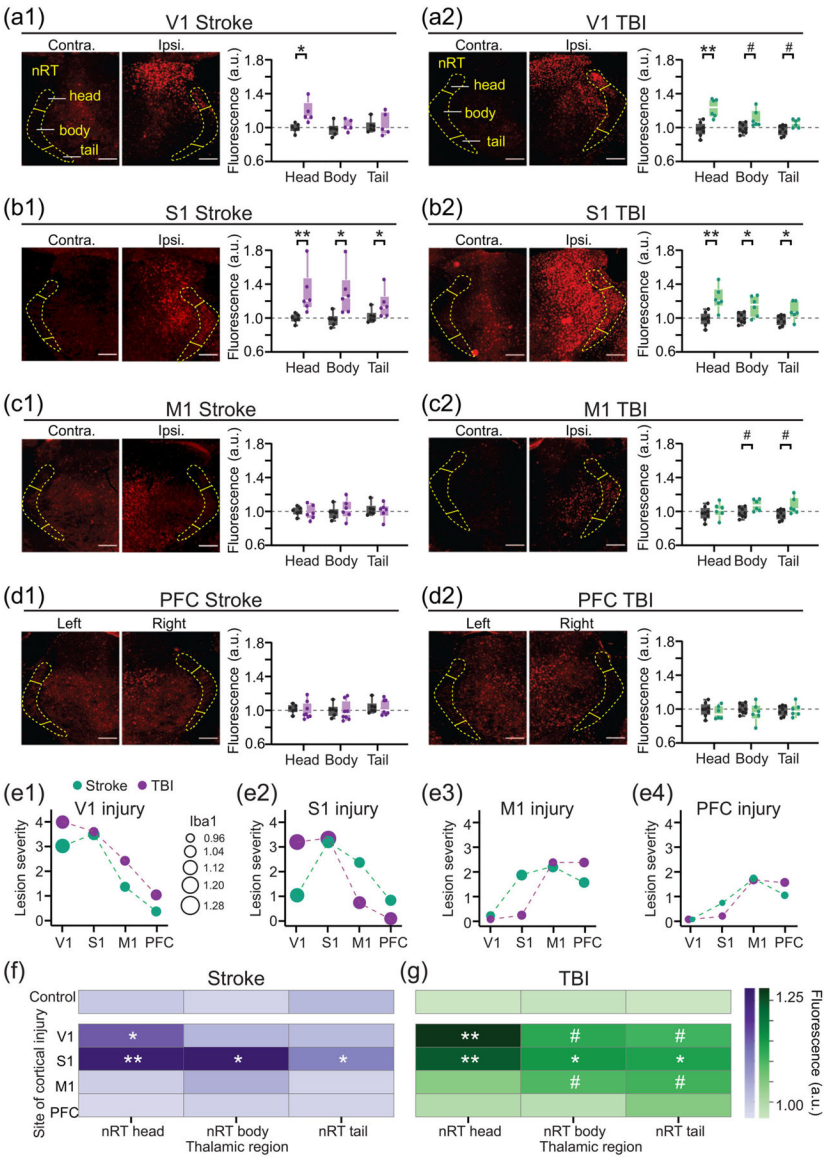


**FIGURE 7.**

Microgliosis in the nRT following induction of stroke or TBI to different cortical sites mirrors functional corticothalamic connectivity. (a1, b1, c1, and d1) Microgliosis in the head, body, and tail of the nRT after cortical stroke, assessed by raw integrated pixel density taken as a ratio of ipsilateral to contralateral. The nRT is traced in yellow to designate it as a GABAergic structure. Significance was assessed by Mann–Whitney tests using $\alpha = 0.05$ and multiply corrected by the Holm–Sidak method (*$p < .05$, **$p < .01$, $^{\#}p < .05$ without multiple comparison correction). Data are represented by Tukey boxplots with whiskers extending to 1.5*IQR from the first and third quartiles. Scale bars: 300 $\mu$m. $n = 5$–8 mice per targeted injury site. Lesion severities in the region of impact are as follows, from top to bottom: 4,3,4,0. Note that the field of view in 7b1 and 5c1 is the same as that of Figures 5b1 and 7c1, respectively. (a2, b2, c2, and d2) Microgliosis in the head, body, and tail of the nRT after cortical TBI. Apart from injury type, all other figure parameters in (a1–d1) also

apply. Lesion severities in the region of impact are as follows, from top to bottom: 3,3,2,3. (e1–e4) Bubble plots representing lesion severity by cortical site together with inflammation in the corresponding region of the thalamus (V1: nRT head, S1: nRT body, M1: nRT tail, and PFC: nRT tail). Bubble size represents Iba1 fluorescence. Each panel heading represents the site at which cortical injury was induced, while the x-axis indicates the cortical regions in which lesion severity was analyzed. For detailed explanation, please refer to the legend of Figure 5e1–e4. (f) Sham-normalized heatmap summarizing results from (a1–d1). (g) Sham-normalized heatmap summarizing results from (a2–d2)

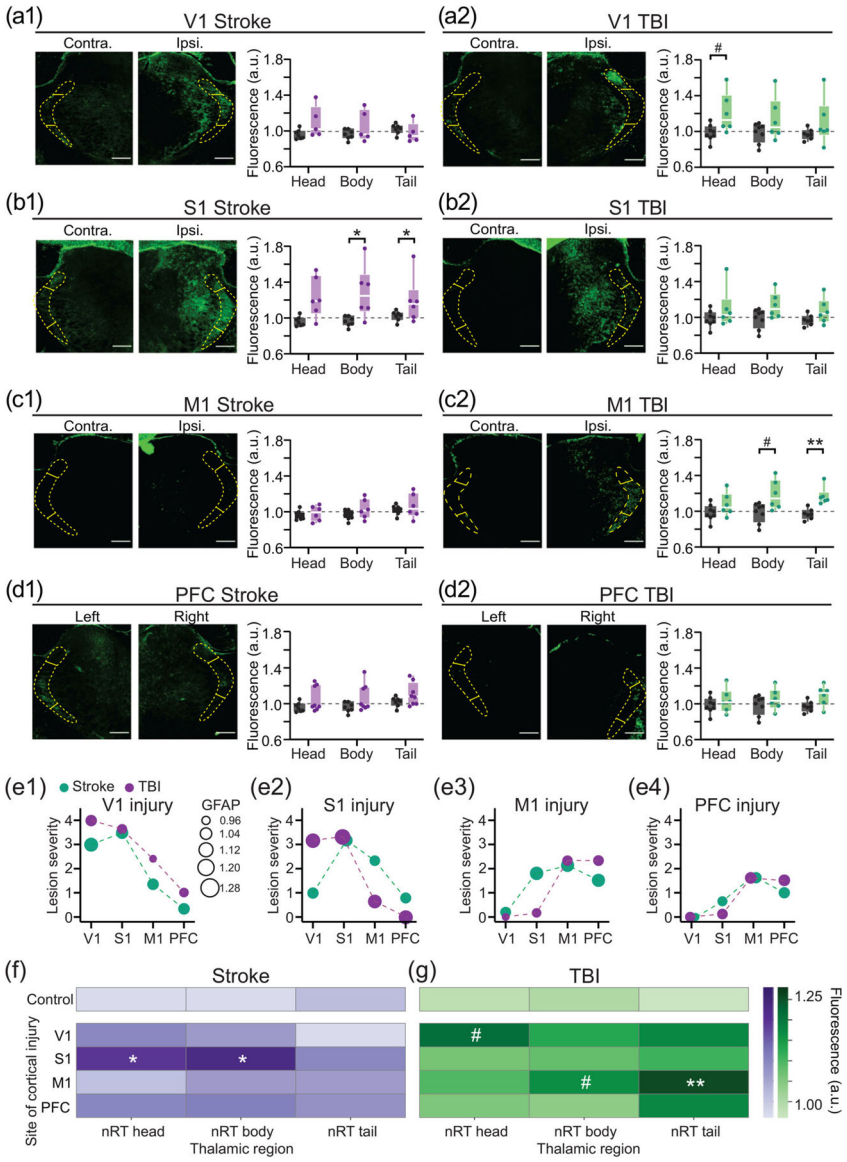


**FIGURE 8.**

Astrogliosis in the nRT following induction of stroke or TBI to different cortical sites mirrors functional corticothalamic connectivity. (a1, b1, c1, and d1) Astrogliosis in the head, body, and tail of the nRT after cortical stroke, assessed by raw integrated pixel density taken as a ratio of ipsilateral to contralateral. The nRT is traced in yellow to designate it as a GABAergic structure. Significance was assessed by Mann–Whitney tests using $\alpha = 0.05$ and multiply corrected by the Holm–Sidak method (*$p < .05$, **$p < .01$, $^{\#}p < .05$ without multiple comparison correction). Data are represented by Tukey boxplots and whiskers extending to 1.5*IQR from the first and third quartiles. Scale bars: 300 $\mu$m. $n = 5$–8 mice per targeted injury site. Lesion severities in the region of impact are as follows, from top to bottom: 4,3,2,2. Note that the field of view in 8b1 is the same as that of Figure 6b1. (a2, b2, c2, and d2) Astrogliosis in the head, body, and tail of the nRT after cortical TBI. Apart from injury type, all other figure parameters in (a1–d1) also apply. Lesion severities in the region

of impact are as follows, from top to bottom: 3,4,3,1. Note that the field of view in 8b2 is the same as that of Figure 6b2. (e1–e4) Bubble plots representing lesion severity by cortical site together with inflammation in the corresponding region of the thalamus (V1: nRT head, S1: nRT body, M1: nRT tail, and PFC: nRT tail). Bubble size represents GFAP fluorescence. Each panel heading represents the site at which cortical injury was induced, while the x-axis indicates the cortical regions at which lesion severity was analyzed. For detailed explanation, please refer to the legend of Figure 5e1–e4. (d) Sham-normalized heatmap summarizing results from (a1–d1). (e) Sham-normalized heatmap summarizing results from (a2–d2)

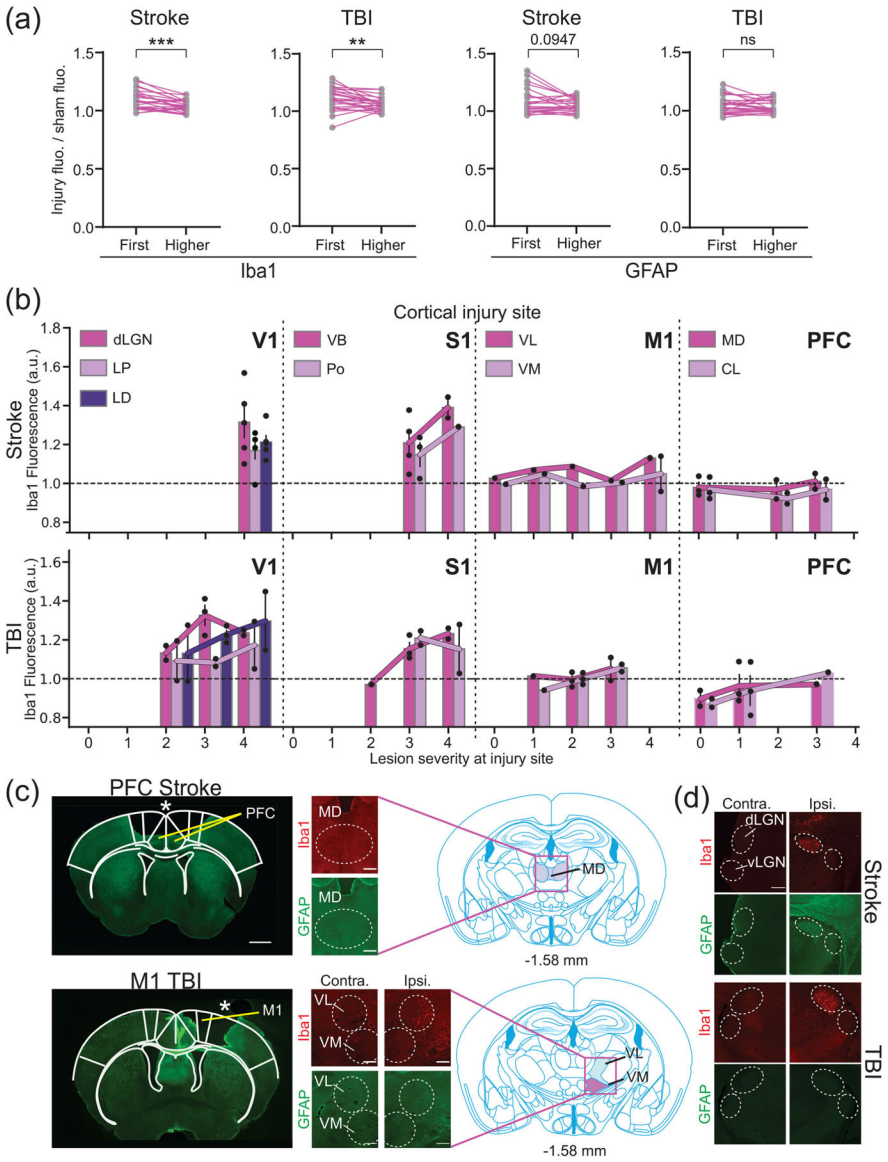


**FIGURE 9.**

Vulnerability of first versus higher order thalamic nuclei. (a) "Before-and-after" plots contrasting the injured/sham fluorescence ratio between first and higher order thalamic nuclei after stroke and TBI. First order nuclei: dLGN, VB, and VL. Higher order nuclei: LP, LD, Po, VM, MD, and CL. Significance was assessed by paired *t*-tests using $\alpha = 0.05$ (**$p < .01$, ***$p < .001$, ns $p > .05$). $n = 25$ mice per "before" and "after" in each comparison. (b) Bar-and-line plots illustrating the correlation between lesion severity and Iba1 fluorescence in the corresponding thalamic region (V1: visual, S1: somatosensory, M1: motor, and PFC: limbic). $n = 1–5$ per bar. (c) (left) Low magnification coronal brain section with PFC stroke and low magnification coronal brain section with M1 TBI. Lesion severities are graded at 3 for both the M1 and PFC sections. White asterisk indicates the lesion site. Scale bar: 1 mm. (right) Close-up images of the low magnification Iba1- and GFAP-labeled brain sections with relevant regions of interest in the limbic and motor thalamus demarcated. Scale bar:

300 μm. Atlas images represent the approximate bregma coordinate at which the close-up images were sourced with the approximate field of view outlined. (d) Representative close-up images of micro- and astrogliosis, labeled by Iba1 and GFAP, respectively, in the ventral lateral geniculate nucleus (vLGN) relative to the dLGN after V1 stroke and TBI of any severity. Scale bar: 300 μm